Engineered Science
DOI: https://dx.doi.org/10.30919/es1488

Utilizing Partially Filled Inner Electron Centers: An Overview of their Enhanced Photocatalysis for Energy and Environmental Applications

Jinshan Xue,[1, 2,#] Can Jin,[1, 2,#] Liquan Jing,[1, 2, 3,*] Zheng Li,[3] Pandeng Li,[3] Hui Wang,[3] Zhanhua Huang[1, 2,*] and Jinguang Hu[3,*]

Abstract

Photocatalysis technology has attracted much attention in the fields of energy and environment, the core of which is the design of photocatalyst. In the past decade, improving performance by changing the internal electronic structure has attracted attention, especially the d-band (p-band) center manipulation, which is mainly used in photocatalytic hydrogen production and CO_2 reduction. In photocatalysis, the d-band (p-band) center of photocatalysts is analyzed by theoretical calculation, which is crucial for photon absorption, electron-hole pair generation, charge separation, transportation, and targeted surface catalytic reactions. By manipulating the d-band (p-band) centers through element doping and other means, the overall electron distribution of the photocatalysts is affected, so that it has a great impact on the adsorption of small molecule intermediate products, optimize and change the reaction path, and realize the improvement of the photocatalytic performance. The objective of this review is to furnish a thorough overview on this topic for a diverse audience. It introduces the advantages of the d-band (p-band) center strategy, explores its correlation with the photocatalytic mechanism, elucidates methodologies for introducing these centers, and discusses existing challenges and potential future prospects in the field.

Keywords: d-band center; p-band center; Photocatalysis; Design.
Received: 25 March 2025; Revised: 15 April 2025; Accepted: 06 May 2025.
Article type: Research article.

1. Introduction

Environmental pollution and energy crisis issues have become a top priority around the world.[1,2] Therefore, there is an urgent need to obtain sustainable green energy to deal with the above issues.[3-11] Solar energy has invited a great deal of interest as a clean, green, abundant, and cheap energy. As an emerging innovative oxidization technology, photocatalytic technology has been widely sought after and is a potential green way to solve environmental and energy problems.[12-21] Nowadays, photocatalytic technology is primarily applied in the fields of environmental restoration and energy conversion, and the kernel of photocatalytic reaction is photocatalyst.[22-25] Therefore, the design of efficient new photocatalysts (strong photoredox ability, efficient charge migration, rapid surface reaction) has become a study hotspot to deal with the above two major problems.[26-29]

In the past decade, photocatalyst modification strategies have been developed significantly, not only greatly improving performance but also diversifying the modification methods. Among them, more and more attention has been paid to enhancing the performance of photocatalysts by modifying their internal electronic structures, with a special focus on manipulating the d-band (p-band) centers. The d-band (p-band) center can affect the electronic structure of photocatalytic materials, the separation and migration of e^--h^+ pairs, the adsorption and reactivity of surface molecules, and the overall reaction efficiency of photocatalysis, *etc*.[30-37] There are multiple interactions in the d-band (p-band) central model, such as metal-small molecule reactant interactions, electron-metal ion interactions, metal-metal interactions, and charge

[1] *State Key Laboratory of Utilization of Woody Oil Resource, Northeast Forestry University, Harbin, 150040, China*
[2] *Key Laboratory of Bio-based Material Science and Technology, Ministry of Education, Material Science and Engineering College, Northeast Forestry University, Harbin, 150040, China*
[3] *Department of Chemical and Petroleum Engineering, University of Calgary, 2500 University Drive, NW, Calgary, Alberta, T2N1N4, Canada*
[#] *These authors contributed equally.*
**Email:* liquan.jing@ucalgary.ca (L. Q. Jing); huangzh1975@163.com (Z. H. Huang); jinguang.hu@ucalgary.ca (J. G. Hu)

transfer interactions, which together regulate the adsorption, activation, and catalytic properties of materials. Among them, the change of the center position of the d-band (p-band) has a great impact on the interaction between the transition metal surface and small molecules, which can enhance the adsorption ability of the transition metal to small molecules, and improve the adsorption selectivity of different small molecules, thus affecting the reaction activity. In addition, electron transfer occurs between the transition metal surface and small molecules. In short, the d-band (p-band) center is closely related to photocatalytic performance because it furnishes novel insights into the electronic structure and reactivity of catalyst materials. By understanding and manipulating the location of the d-band (p-band) center, researchers can improve the efficiency of the photocatalytic process. Currently, people are still mainly focusing on the extensive use of d-band center regulation in photocatalysis, and the regulation of p-band centers is beginning to be paid attention to, and it is possible that the application of f-band center regulation in photocatalysis will begin to be paid attention to in the future. In general, the regulation of the position of the inner electron center can play a significant function in photocatalysis.

In order to explore the relationship between the d-band (p-band) centers and photocatalytic performance of catalysts, the objective of this review is to comprehensively summarize the recent research progress of d-band (p-band) center regulation in photocatalysis. First, the reaction mechanism of d-band (p-band) center and its consequence on the photocatalytic process. In addition, we discuss the relation between the moving direction of the d-band (p-band) center position and the catalytic reaction. Subsequently, we discuss the current means of characterizing the d-band (p-band) center. Finally, we summarize the current means of regulating the location of the d-band (p-band) center, including doping, defects/vacancies, heterojunction, alloying, and stress, *etc*. In conclusion, we summarize the current research status and problems of d-band (p-band) center, and look forward to the future prospects as well as challenges for the application of d-band (p-band) center in photocatalysis. This research provides a key theoretical basis for understanding the relationship between electronic structure and performance of catalysts, deeps the understanding of the structure-activity relationship of materials, theoretically promotes the further development of photocatalysis from empirical exploration to rational design, thus promoting the green transformation of industry, and has important scientific significance for the field of photocatalysis to industrial practical application.

2. The impact of d-band (p-band) center on photocatalytic reactions

2.1 Functions and advantages

Fig. 1a shows the distribution of active inner-layer electrons in the periodic table of elements. Active d-layer electrons are mainly concentrated in the transition metal region, active p-layer electrons are mainly concentrated in several main group regions, and active f-layer electrons are mainly concentrated in some elements of the lanthanide and actinide series. Figs. 1b-c shows the distribution of electrons in the outer layers of elements in the periodic table. Electrons closer to the nucleus have lower energy. As the number of electron layers increases, the energy of the electrons becomes larger and larger. Next, the partial reaction principles of d-band center (main) and p-band center will be introduced.

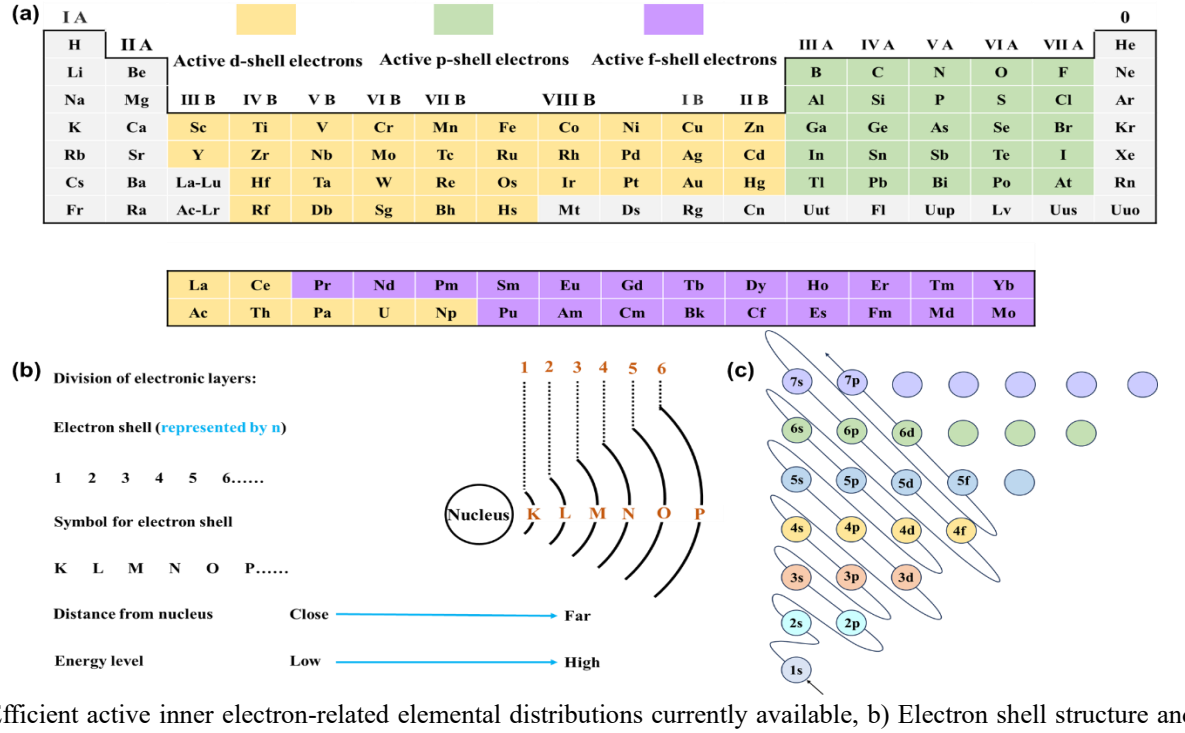

Fig. 1: a) Efficient active inner electron-related elemental distributions currently available, b) Electron shell structure and energy, and c) The arrangement of electrons outside the nucleus.

The d-band center model essentially describes the interaction between the transition metal surface and a small molecule. It results in the mixing of the transition metal's d-band with the orbitals of the small molecule, resulting in the establishment of antibonding and bonding states, as illustrated in the accompanying Fig. 2a.[38-40] In this depiction, the orange and grey colors represent occupied and unoccupied states, respectively, with ε_F denoting the Fermi energy level. All states below ε_F are occupied, while bonding states are always completely inhabited, and antibonding states are partly inhabited. Firstly, the energy level of the d-band center decides the grade to which the antibonding energy band is filled with electrons, affecting the strength and stability of adsorption bonding, known as the d-band center theory. An upward shift of the d-band center towards the Fermi energy level generally leads to stronger reactant adsorption. When analyzing the periodic table, among metallic elements in the same period, the d-band center consistently rises from right to left, resulting in enhanced adsorption. Additionally, the d-energy bands corresponding to the valence electrons of each element group exhibit a gradual weakening of coupling strength from top to bottom, along with a monotonically decreasing adsorption energy. Secondly, the d-band center influences a catalyst's capability to activate and dissociate reactant molecules. Furthermore, d-band centers can impact the selectivity of catalytic reactions by determining the preferential binding and activation of specific reactant molecules. Lastly, the kinetics of catalytic reactions, including reaction rates and activation energy barriers, are also influenced by d-band center positions. Favorable d-band centers can lower activation barriers, consequently accelerating reaction rates. It is important to note that the specific effects of d-band centers may vary depending on the catalyst's composition, structure, as well as the nature of the reactants and reactions involved. Researchers often customize catalysts by manipulating d-band centers to optimize their performance for specific catalytic applications.

The d-band center theory plays a substantial function in photocatalytic performance, which is closely relevant to the electronic structure of the catalyst and the adsorption ability of the reactant molecules and their intermediates.[41-43] The binding energies of the reactant molecules and intermediates can be changed by adjusting the situation of the d-band center of the transition metal in the catalyst. d-band center position affects the light absorption ability and charge separation efficiency of the catalyst. When the d-band center is near to the Fermi energy level, the trapping ability of photogenerated charge can be enhanced, therefore ameliorating the photocatalytic efficiency. In some cases, adjusting the d-band center not only affects the photocatalytic performance but also the reaction selectivity. Lattice strain engineering can modulate the interaction of the catalytic surface with adsorbate molecules by changing the electronic and geometrical configurations of the metal sites, thus affecting the situation of the d-band center and the photocatalytic performance. The combination of theoretical calculations, such as density-functional theory (DFT) calculations, which predict the trend of the d-band centers, and experimental studies, which validate the theoretical predictions, can provide insights into the influence of the d-band centers on photocatalytic performance. Understanding the relation between the d-band center and the photocatalytic performance helps to design and develop new and efficient photocatalytic materials. Optimization of photocatalytic reaction activity and selectivity can be achieved through precise tuning of the d-band center. d-band center and physical quantities such as the figure of merit are both expressions of the electronic properties of metals and are both used as descriptors for the understanding of the electrocatalytic activity of metals. However, they describe the electronic structure and catalytic activity of metals from different perspectives. Through the above points, we can see the importance of the d-band center in the photocatalytic performance and that the performance of the catalyst can be effectively optimized through modulating the d-band center. Nevertheless, this theory also needs to be combined with other factors and effects to fully understand and design efficient photocatalytic materials.

The p-band center theory is an important concept in the science of catalysis, especially playing a significant function in the design and understanding of catalysts containing nonmetals.[44-48] The situation of the p-band center is often used to describe the ability of the catalyst to interact with the reactants. In nonmetal-containing catalysts, the position of the p-orbital center can be applied as a descriptor to assess their catalytic activity. Modulation of the hybridization mode and occupancy state of the p orbitals of nonmetallic atoms by changing dimensions and sizes, elemental doping, and material composites can activate the p electrons and thus modulate the activity of the catalyst. The correlation between the adsorption properties of nonmetallic active centers and the p-orbital properties provides an important guidance for the precise design of highly active nonmetallic catalysts. Through theoretical calculations and experimental characterization, the origin and induction mechanism of the catalytic activity dominated by p orbitals can be revealed, so as to understand the relation between the catalytic activity and electronic structure of catalysts. p-band center theory provides a universal idea that p electrons can be activated for various types of catalytic reaction systems by modulating the hybridization mode and occupancy state of the p orbitals of nonmetallic atoms. This theoretical knowledge demonstrates the important role of p-band centers in catalyst design and catalytic reactions, especially in the development of nonmetal-containing catalysts. p-band center theory provides an effective tool for understanding and predicting catalyst performance.

The relationship between p-band centers and photocatalytic performance is multifaceted and involves the electronic structure of the catalyst as well as the interaction with the reactants.[44,49,50] In the photocatalytic process, the position of the p-band center is usually used to describe the

interaction ability between the catalyst and the reactants. p-band center position influences the electronic structure of the catalyst surface, which in turn influences the adsorption and desorption behaviors of the target intermediates. p-band center position can affect the light absorption capability and charge separation efficiency of photocatalytic materials. It is mentioned that the band gap size and energy band structure have a substantial consequence on the activity of photocatalytic reactions, and the position of the p-band center affects these electronic structure properties. In composites, the modulation of the p-band center can achieve better migration and separation of photogenerated carriers, thus boosting the photocatalytic activity. Understanding the relationship between p-band centers and photocatalytic properties can help to design and develop new and efficient photocatalytic materials. In conclusion, the p-band center plays a cardinal part in the photocatalytic performance, which influences the electronic structure, light absorption ability, charge separation efficiency, and interaction with the reactants of the catalyst, and thus the overall photocatalytic efficiency. Through theoretical analysis and experimental studies, the p-band center can be effectively regulated to improve the performance of photocatalytic materials.

Figs. 2b-f demonstrate the five main types (dp type, p1p2 type, d1d2p type, dp1p2 type, p1p2p3 type) of photocatalysts in which synergistic modulation between the d-band center and the p-band center can occur. Among them, dp type (*e.g.*, CdS, ZnS, TiO_2, *etc.*), p1p2 type (*e.g.*, BN, C_3N_4, Bi_2O_3, Sb_2S_3, Bi_2Se_3, *etc.*), d1d2p type (*e.g.*, $CoFe_2O_4$, ZnCdS, *etc.*), dp1p2 type (*e.g.*, $CuBi_2O_4$, $ZnIn_2S_4$, $CdIn_2S_4$, $BiVO_4$, *etc.*), p1p2p3 type (*e.g.*, BiOCl, BiOBr, BiOI, $SnIn_4S_8$, BCN, $BiPO_4$, *etc.*), and these photocatalyst types above are almost spread over the whole semiconductor types, in addition to some metal-organic frameworks (MOFs), covalent organic frameworks (COFs), high entropy materials, alloys, and some other new materials have received much attention, and the strategy of d-band center and p-band center modulation can also be used to optimize their photocatalytic performance.

In photocatalytic performance, d-band (p-band) centers are usually discussed rather than f-band centers because the d-band center theory is mainly applicable to transition metal catalysts, whereas f-band centers are related to the catalytic performance of lanthanides and actinides. Although f-band centers are not as common as d-band centers in photocatalysis, it is theoretically possible to affect the electronic structure of the catalysts, which in turn may affect their photocatalytic performance, by modulating the arrangement and energy levels of the f electrons. Under some specific conditions, the situation of the f-band center may affect the catalyst's interaction with photoexcited electrons and thus the separation and movement efficiency of photogenerated charge carriers. Similar to the d-band center theory, the f-band center may be related to the spin-polarized state of the catalyst, which may affect the complexation process of photogenerated e^- and h^+, and thus the catalytic efficiency. For catalysts containing lanthanides or actinides, the location and properties of the f-band center may have a direct influence on the adsorption and activation of redox reaction intermediates. Although the f-band center is not a conventional descriptor in photocatalysis, considering the properties of the f-band center when designing specific types of photocatalytic materials may help to optimize the performance of the materials.

2.2 Effect of d-band (p-band) center position on photocatalytic reaction

2.2.1 d-band center upward shift

Shifting the d-band center upwards in photocatalytic materials can also have a variety of effects on their photocatalytic

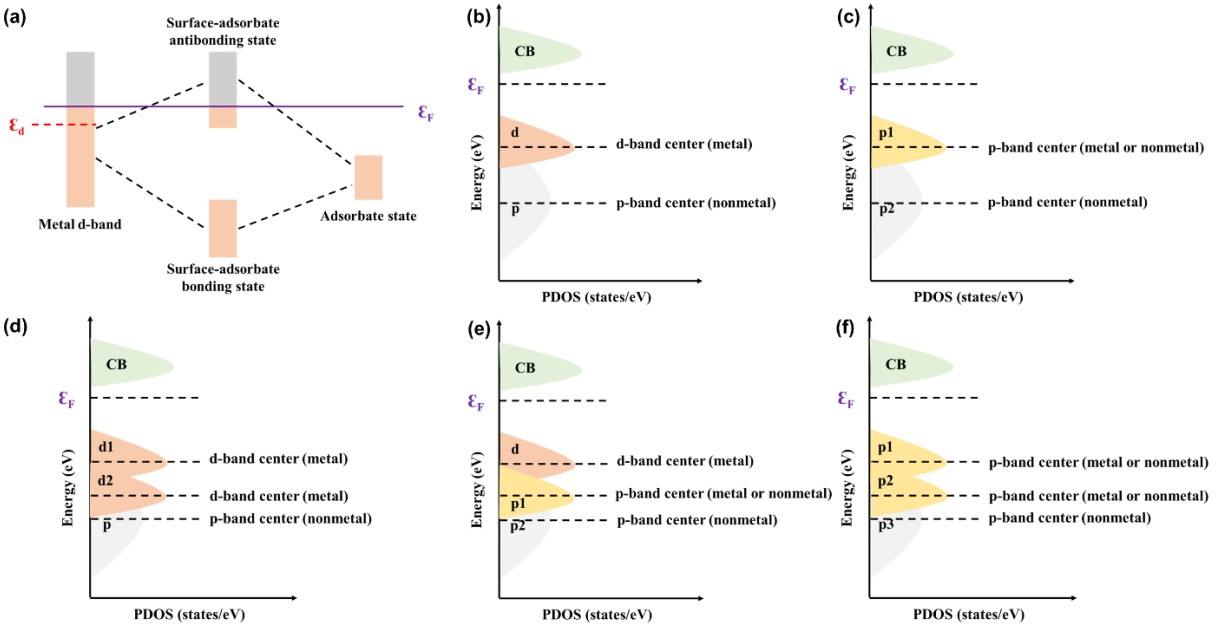

Fig. 2: a) Model diagram of d-band center metal surface adsorbing reactants, b-f) Model diagrams of several current different d-band (p-band) centers and the hybrid types between them.

activity, and some of the main potential effects of upward shifting of the d-band center in the photocatalytic context are: alteration of carrier kinetics, alteration of redox potentials, enhancement of adsorption, and improvement of the selectivity of some of the reactions (in some cases, upward shifting of the d-band center can be intentionally designed to optimize photocatalysts for a particular reaction. It can enhance the selectivity of the material for some photocatalytic reactions while reducing its activity for others, *etc*. Overall, the influence of upward shifting of the d-band center on photocatalysis may vary relying on the specific photocatalyst, the photocatalytic reaction being investigated, and the desired outcome.[51-55] However, the main photocatalytic reactions (CO_2 reduction (most), N_2 fixation, biomass conversion, hydrogen production (heterojunctions/homojunctions), oxygen production, *etc*.) still utilize the upward movement of the d-band center of the photocatalytic material to facilitate the reaction. Hu *et al*. explored the electronic interaction between $WO_{2.72-x}$ and Fe single atoms and how this interaction affects the photocatalytic performance, especially in the photoreduction N_2.[56] DFT calculations on the d-band center in Fig. 3a show that the electronic interaction between $WO_{2.72-x}$ and the Fe single atom leads to a shift of the d-band center toward the Fermi energy level, and this shift enhances the bonding of N_2 to the catalyst surface. The upward shift of the d-band center increases the Fermi antibonding states above the energy level, which enhances the adsorption of N_2. This is because the upward shift of the d-band center means that more electronic states are located above the Fermi energy level, which contributes to the adsorption and activation of N_2 molecules.

Further, the adsorption sites of N_2 on $WO_{2.72}$, $WO_{2.72-x}$, and Fe-SA/$WO_{2.72-x}$ were diverse, and the most favorable N_2 adsorption energy was found on Fe-SA/$WO_{2.72-x}$, which indicated that the introduction of Fe single atoms significantly enhanced the N_2 adsorption capacity (Fig. 3b). In conclusion, the electronic interactions between $WO_{2.72-x}$ and Fe single atoms enhanced the N_2 adsorption and activation by regulating the situation of the d-band centers, thus improving the performance of photocatalytic nitrogen reduction. Feng *et al*. constructed a method to modulate the kinetics of photocatalytic CO_2 reduction reaction by modification of surface coordination spheres.[57] DFT calculations in Fig. 3c show that by modifying isolated Mn atoms on polygonal TiO_2 nanobubbles (TONP) (forming Mn/TONP), the d-band center can be up-regulated, which facilitates the adsorption of CO_2. The upward shift of the d-band center implies that more electronic states are located above the Fermi energy level, which contributes to the adsorption and activation of CO_2 molecules. The possible pathways for the conversion of CO_2 to CO were investigated by calculations of free energy diagrams (Fig. 3d), and it was found that the Mn site not only favors the adsorption of CO_2, but also significantly lowers the energy barrier for the constitution of *COOH and accelerates the decisive step of the reaction.

In conclusion, Mn/TONP as an effective catalyst for CO_2 photoreduction was confirmed by experiments and DFT calculations, and the modified Mn atoms not only enhanced CO_2 adsorption by optimizing the d-band centers, but also acted as an active site to significantly lower the reaction energy barrier of the deceleration step of CO_2 reduction, which achieved the unity of adsorption and activation. Ni *et al*. improved the efficiency of photocatalytic CO_2 methanation by constructing a direct Z-scheme and introducing specific types of oxygen vacancies (V_{Os}) in Co_3O_4/$NiCo_2O_4$ heterogeneous nanocages (HNCs).[58] The introduction of Ni atoms was capable to modulate the electronic constitution of $NiCo_2O_4$, bringing the d-band centers around the Co atoms nearer to the Fermi energy level, which contributes to the hydrogenation procedure at the V_{O2} site, which enhanced the adsorption and activation of CO_2 (Fig. 3e). Further, the CO_2 hydrogenation processes on different V_O sites on the $NiCo_2O_4$ surface were analyzed by theoretical calculations (Fig. 3f). The calculations showed that the V_{O2} sites significantly reduced the formation energy of the COOH intermediate state, favoring the conversion of CO_2 to COOH. For the $NiCo_2O_4$-V_{O2} model, the *CHO intermediate state was energetically favored over the pathway of generating CO, and further hydrogenation could generate CH_4. Moreover, the V_{O2} sites were able to generate CO_2 to CH_4 after its conversion to CO_2 by combining with electrons and protons to form the hydroxyl group (*OH), which then easily detaches from the $NiCo_2O_4$ surface, enabling self-regeneration of the V_{O2} vacancy.

Overall, the introduction of Ni atoms and the presence of specific V_{O2} vacancies not only changed the selectivity of CO_2 photoreduction, but also realized an efficient and stable methanation process and maintained the long-term stability of the photocatalysts through the self-regeneration mechanism. Sun *et al*.[42] improved the CO_2 photoreduction efficiency by d-band center modulation of copper atom sites in phosphorus-doped carbon-nitride (PCN) structures. The results of the DFT showed that the d-band center of the copper atom was shifted upward and closer to the Fermi energy level when the phosphorus atom replaced a carbon atom in C_3N_4. This upshift enhances the adsorption and activation of CO_2 on the sites of the copper atoms, thereby increasing the efficiency of CO_2 conversion to CO. Further, DFT calculations also reveal that the CO_2 photoreduction reaction's rate-determining step (CO_2* + H^+ + e^- → COOH*) has a significantly lower reaction energy on Cu_1N_3@PCN, suggesting that this step is easier to carry out (Fig. 3g). Overall, the doping of phosphorus atoms shifted the d-band center of copper atoms upward, which enhanced the adsorption and activation of CO_2, thus improving the efficiency of CO_2 photoconversion to CO.

2.2.2 d-band center downward shift

Shifting the d-band center downward in photocatalytic materials can also affect their photocatalytic activity in various ways. Some of the main potential effects of d-band center downward shifting in the photocatalytic context are: change of

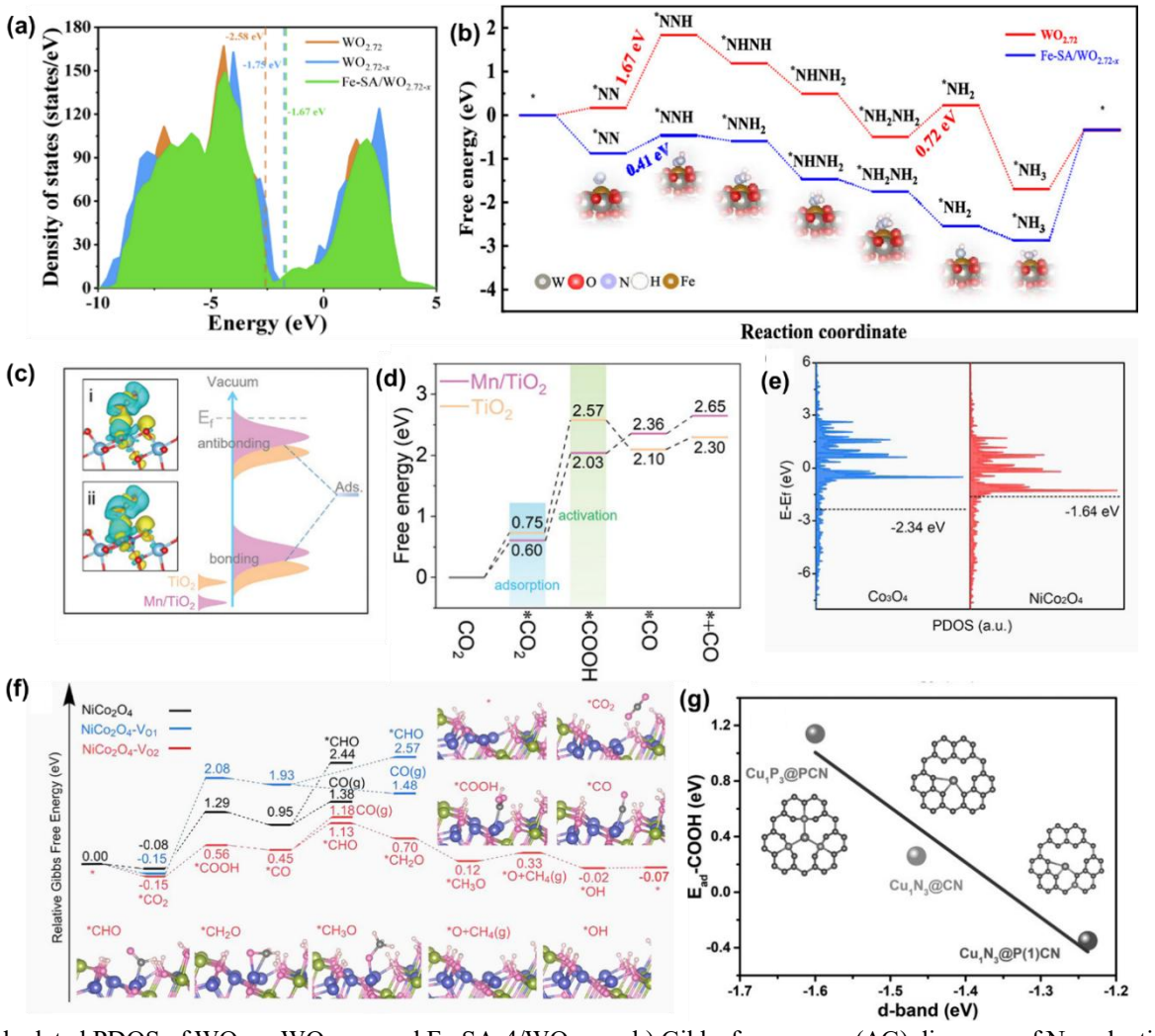

Fig. 3: a) Calculated PDOS of $WO_{2.72}$, $WO_{2.72-X}$ and Fe-SA-4/$WO_{2.72-X}$, b) Gibbs free energy (ΔG) diagrams of N_2 reduction to NH_3 by distinct routes on $WO_{2.72}$ and Fe-SA/$WO_{2.72-x}$, a-b reproduced with the permission from [56], Copyright 2022 American Chemical Society. c) The calculated distinguishing charge density of CO_2 molecule absorbed on i: TiO_2 and ii: Mn/TiO_2, and homologous schematic chart of bond formation between the catalyst surface and the adsorbate, d) The calculated free energy charts for the conversion of CO_2 into CO on TiO_2 and Mn/TiO_2, c-d reproduced with the permission from [57], Copyright 2023 Wiley. e) Incomplete density of states for the adsorption site (Co atom) on Co_3O_4-V_{O2} and $NiCo_2O_4$-V_{O2} surfaces, and the d-band center, f) Reaction route for CO_2 photocatalysis on the $NiCo_2O_4$ surface with and without distinct V_O. The Ni, O, Co, C, and H atoms are depicted through prasinous, pink, violet, gray, and white balls, respectively, e-f reproduced with the permission from [58], Copyright 2023 American Chemical Society. g) The relation between adsorption energy of COOH* on single Cu sites of three model catalysts and d-band center, g reproduced with the permission from [42], Copyright 2022 Wiley.

the electronic structure, enhancement of light absorption, enhancement of the carrier mobility, enhancement of the stability, weakening of adsorption capacity, and improvement of the selectivity of part of the reaction (much higher rate of the generation of desorption-like products), and so on. Overall, the exact effect of the downward shift of the d-band center on photocatalysis will depend on the specific material and the expected photocatalytic reaction.[59-62] However, the main photocatalytic reactions that can be promoted by the downward shift of the d-band center of photocatalytic materials are H_2 production (co-catalyst modulation), H_2O_2 production, and degradation. Qiao *et al*. prepared carbon-doped molybdenum disulfide/molybdenum dicarbide (MoO_2/Mo_2C-C) as a co-catalyst for the photocatalytic water decomposition reaction for hydrogen production.[63] The electronic structure of the MoO_2/Mo_2C-C co-catalyst, particularly the situation of the d-band center, was analyzed by DFT (Figs. 4a-b). The downward shift of the d-band center helps to reduce the kinetic barrier of the hydrogen generation reaction, which improves the efficiency of photocatalytic H_2 production.

In the result plot of photocatalytic hydrogen production performance in Fig. 4c, the MoO_2/Mo_2C-C co-catalyst combined with CdS significantly increased the rate of photocatalytic hydrogen production to 18.43 $mmol \cdot g^{-1} \cdot h^{-1}$, which is close to the hydrogen production performance of Pt-CdS (19.58 $mmol \cdot g^{-1} \cdot h^{-1}$). This work supplies an in-depth study of the performance of MoO_2/Mo_2C-C co-catalysts in

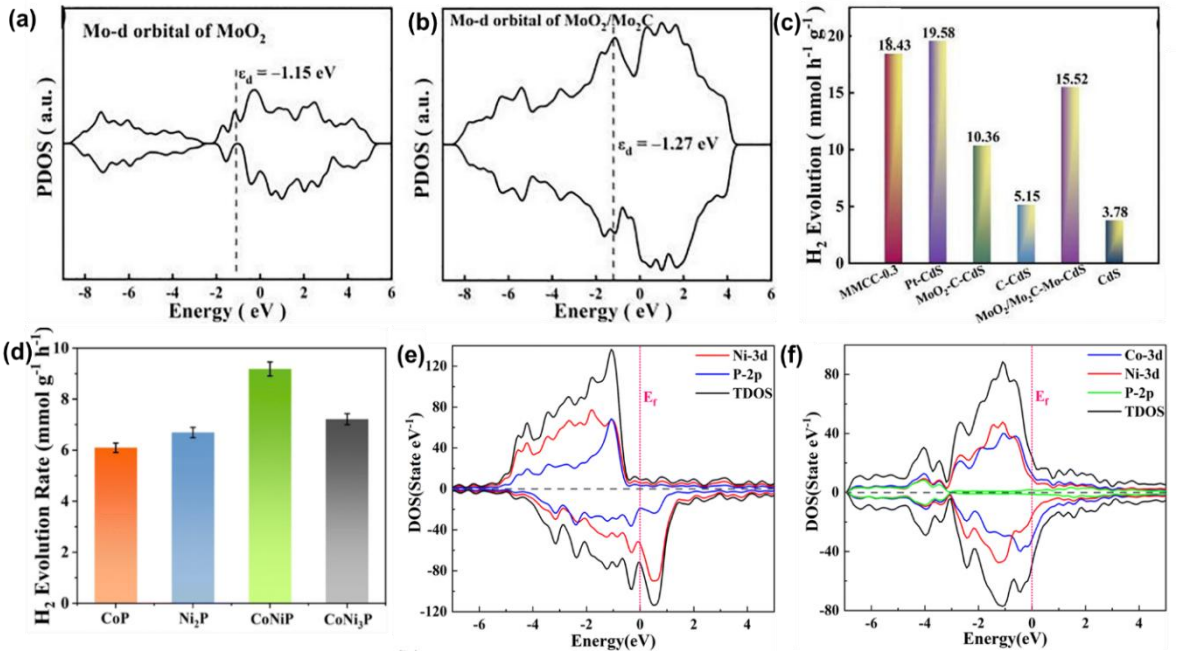

Fig. 4: a-b) d-band center of MoO_2 and MoO_2/Mo_2C cocatalyst, c) Activity comparison of diverse catalysts including C-CdS, MoO_2/Mo_2C-Mo-CdS and MoO_2-C-CdS, a-c reproduced with the permission from [63], Copyright 2023 Elsevier. d) Photocatalytic H_2 evolution activities of CoP, Ni_2P, CoNiP and $CoNi_3P$ through using eosin-Y (5 mg) and catalysts (2.5 mg), e-f) Total electron density of states (DOS) of Ni_2P and CoNiP, which protruded on Ni, Co and P atoms. The Fermi level is fixed as zero. d-f reproduced with the permission from [64], Copyright 2023 Royal Society of Chemistry.

photocatalytic hydrogen production through a conjugation of theoretical calculations and experimental methods, especially the optimization of the electronic structure of the co-catalysts through adjusting the d-band centers, which improves the efficiency and stability of the photocatalytic hydrogen production. Cheng *et al*. constructed precious metal-free ternary cobalt-nickel phosphides (CoNiP) for photocatalytic dye-sensitized H_2 production and investigated their catalytic mechanism.[64] The experimental results showed that CoNiP displayed the most excellent activity in the photocatalytic hydrogen evolution for dye sensitization (Fig. 4d), reaching 12.96 $mmol \cdot g^{-1} \cdot h^{-1}$, which was mainly imputed to the excellent electrical conductivity and low hydrogen precipitation overpotential of the phosphides, which originated from their metallic properties and the presence of free electrons, which facilitated the efficient electron transfer between the catalyst and sensitizer. Further, DFT calculations disclosed that CoNiP's d-band center position is more negative than that of Ni_2P, which implies that CoNiP has a weaker adsorption capacity for H_2 molecules and thus is more favorable for hydrogen generation (Figs. 4e-f). Overall, the electronic structure of the co-catalyst was optimized by adjusting the d-band center, which improved the efficiency of photocatalytic H_2 production.

2.2.3 p-band center

The situation of the p-band center in a photocatalyst plays a crucial role in determining its photocatalytic activity. Both upward and downward shifts of the p-band center can have a substantial influence on the performance of the photocatalyst. The situation of the p-band center in a photocatalyst significantly affects its charge separation efficiency, redox properties, and overall photocatalytic performance. While the upward movement of the p-band center commonly boosts the photocatalytic performance by promoting efficient charge separation and surface reactions, the downward movement may have the opposite effect, resulting in a drop-off in performance (which is partly similar to the partial effect of the d-band center). However, the current reports on p-band center-modulated photocatalysts are mainly used for hydrogen production and CO_2 reduction, and the positions of the p-band centers are mainly shifted downward to obtain enhanced photocatalytic effects, which may be related to the reaction paths of the reaction system as well as other influencing factors.[44,49,50,65,66] Therefore, understanding and controlling the p-band center's location is crucial for the optimization and intellectual design of photocatalysts for diverse applications.

3. Characterization of the d-band (p-band) center

In order to establish a clear link to photocatalytic activity, accurate identification of the characteristic structures of the d-band centers (predominantly) and p-band centers is imperative. Fortunately, the advent of cutting-edge technologies in recent years, particularly those capable of analyzing the internal electronic structure of materials at the atomic level, has improved our understanding of materials. Accordingly, accurately determining the d-band center of a catalyst is a complex task that often involves a combination of experimental and theoretical approaches. While no single method is perfect, the accuracy of the assessment can be

improved by using a variety of complementary techniques. In light of this progress, our discussion will focus on several spectroscopic techniques characterization and theoretical calculations that provide evidence for the characteristic structure of the d-band center (Fig. 5). These include X-ray photoelectron spectroscopy (XPS), ultraviolet photoelectron spectroscopy (UPS), electron energy loss spectroscopy (EELS), X-ray absorption near edge structures (XANES), and density functional theory (DFT) calculations. Currently, there are fewer well-tested characterization tests for p-band centers, and the main references are to some of the ways of characterizing d-band centers. The next section focuses on the characterization of d-band centers.

By analyzing the XPS spectra of the catalysts, the researchers can determine the binding energies of the d electrons and other relevant orbitals. The energy difference between the d-band and the Fermi energy level gives an estimate of the d-band center. Fig. 5a illustrates the d-band center locations of different alloys obtained by XPS-VB testing: Ag (-5.28 eV), $Ag_{75}In_{25}$ (-5.51 eV), $Ag_{75}Co_{25}$ (-4.45 eV), $Ag_{75}Fe_{25}$ (-4.71 eV), $Ag_{75}Cu_{25}$ (-5.16 eV). The above results show that the $Ag_{75}Cu_{25}$ alloy has a 0.12 eV upward shift of the d-band center with respect to pure Ag, which contributes to the increase in oxygen reduction activity.[67] The highest oxygen reduction activity was observed for the $Ag_{75}Cu_{25}$ alloy, which indicates that the situation of the d-band center provides the optimum binding energy for the active site, which is neither too strong nor too weak. The UPS can provide information about the position of the Fermi energy level, which is related to the d-band center. By comparing the UPS spectra of different catalysts, the relative location of the d-band center can be inferred. Fig. 5b illustrates the determination of the position of the d-band centers in different Pt3Ni alloys by using UPS.[68]

Specifically, the locations of the d-band centers of Pt_3Ni (111), Pt_3Ni (110), and Pt_3Ni (100) are -3.10 eV, -2.70 eV, and -3.14 eV, respectively. d-band centers on the surfaces of these alloys are all shifted downward compared to the corresponding pure Pt single-crystal surfaces, by 0.16 eV, 0.24 eV, and 0.34 eV, respectively. This shift of the d-band centers is associated with the coordination number of the surface atoms and the interactions between the surface atoms, which influence the sample surface's adsorption capability. By precisely controlling the composition and formation of the alloys, the situations of the d-band centers can be optimized, leading to the design of catalysts with higher catalytic activity. DFT is a computational method used to calculate the electronic structure of a material, which can predict the positions of the electronic energy levels, including the d-band centers, based on the atomic and electronic constitution of the catalyst. Fig. 5c demonstrates the downward shift of the d-band center of CoP from the Fermi energy level due to Ni doping. Specifically, the d-band center of CoP goes down from -1.72 eV to -1.77 eV for Ni-CoP. This downward shift reduces the adsorption energy of hydrogen (H) and contributes to the desorption of hydrogen from the catalyst's surface, which promotes the hydrogen evolution reaction (HER).[69] In summary, the choice of method depends on the specific catalyst, its properties, and the information the researcher seeks to obtain. Typically, a combination of experimental techniques and theoretical calculations is used to gain a comprehensive understanding of d-band centers and their relevance to catalysis, and the advantages and disadvantages of different characterization methods are shown in Table 1.

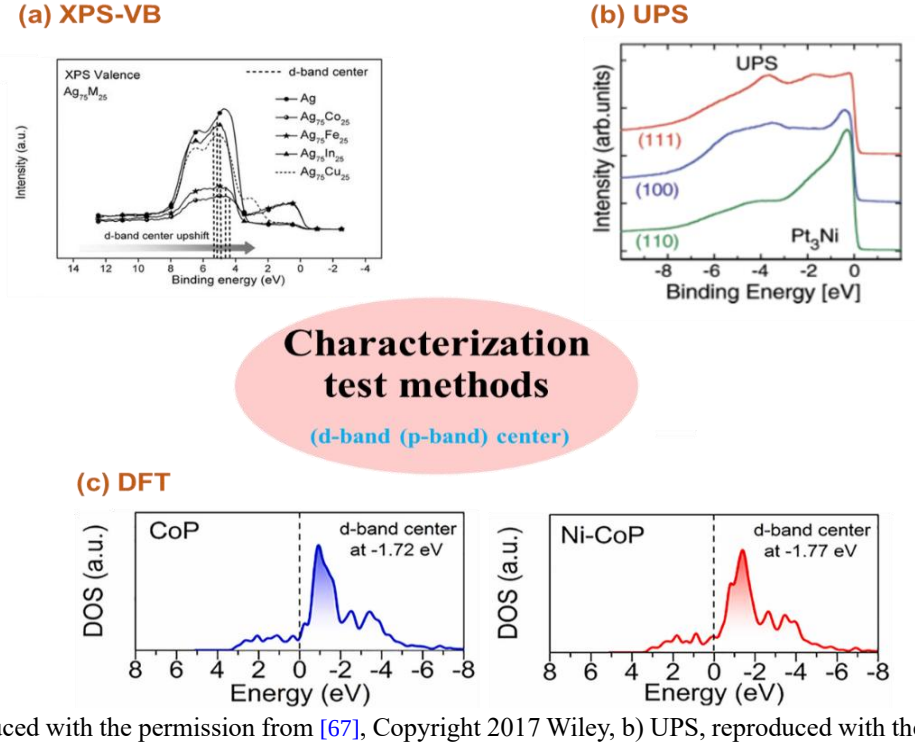

Fig. 5: a) XPS, reproduced with the permission from [67], Copyright 2017 Wiley, b) UPS, reproduced with the permission from [68], Copyright 2007 Science, and c) DFT, reproduced with the permission from [69], Copyright 2019 Elsevier.

Table 1: Comparison of methods for characterizing the d-band (p-band) center.

Characterization methods		Abbreviation	Advantages	Disadvantages
Spectroscopic techniques characterization	X-ray photoelectron spectroscopy	XPS	Accurately analyze the element composition associated with the d-band (p-band) center; Determine the binding energy of the d electron and other associated orbitals	Cause some degree of damage to the sample, and affect the true state of the d-band (p-band) center; Limited resolution
	Ultraviolet photoelectron spectroscopy	UPS	Provide accurate valence electron structure, which is beneficial to study the interaction between d-band (p-band) center and valence electron; Provide the position of Fermi level related to the d-band (p-band) center; High energy resolution	Limited sample applicability; Confined inner electron structure analysis; Complex data processing
	Electron energy loss spectroscopy	EELS	Determine the element chemical environment associated with the d-band (p-band) center; High spatial resolution	Low quantitative analysis accuracy; High sample thickness requirements
	X-ray absorption near edge structures	XANES	Analyze the electronic structure of the d-band (p-band) center and the surrounding atomic environment; High sensitivity and resolution	Harsh experimental conditions; The interpretation of the results depends on a certain theoretical model
Theoretical calculations	Density functional theory	DFT	Calculate the overall distribution of electrons based on electron density; Predict the position of the electron energy level based on the atomic and electron composition of the material, including the d-band (p-band) center	Error existence; High computational cost; Lack of experimental validation

4. Modulation strategy for d-band (p-band) center

As depicted in Fig. 6, the control of the inner electrons of the photocatalysts is mainly the d-band center (about 90% of the share), and the others are the p-band centers. Regarding the control of the d-band center, it is mainly the control of the main catalyst doping (26.7%), followed by the control of the heterojunction (14.7%), and then the modulation of vacancies/defects (13.3%), and the proportion of other control strategies is similar. Currently, there are fewer articles on the modulation of p-band centers of photocatalysts, mainly focusing on strain (13.3%) and modulation of heterojunctions (5.3%). The above results suggest that the modulation of the inner layer of electrons for photocatalysts needs to be further enhanced.

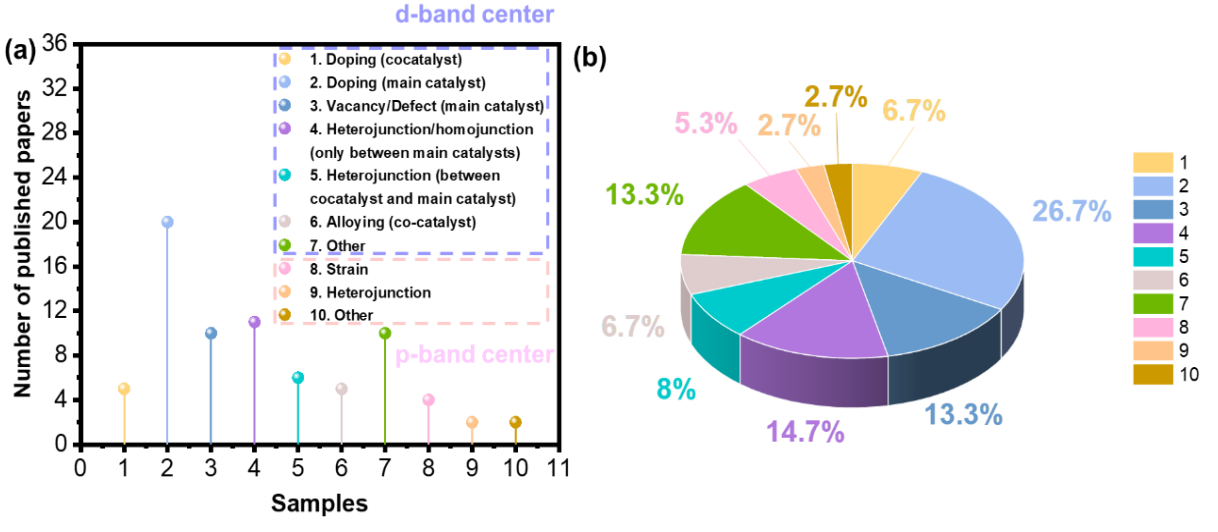

Fig. 6: Publication status (a) and proportion (b) of papers with various modification strategies.

4.1 Modulation strategy for d-band center

4.1.1 Doping (cocatalyst)

The doping of the co-catalyst has a substantial influence on the d-band center as well as the photocatalytic performance.[59,70] The co-catalysts can provide effective active sites for surface reactions and make the surface catalytic reactions easy to occur. Through the migration of photogenerated charges to the co-catalysts, the complexation of photogenerated e^- and h^+ is further inhibited to improve the stability of the photocatalytic system, and the photocatalytic performance of semiconductor nanomaterials is greatly improved. The loading of co-catalysts, especially oxidation and reduction co-catalysts, can markedly improve the activity of catalytic decomposition of water in semiconductor photocatalytic systems. The structure and composition of the co-catalysts have important effects on their performance. In summary, the doping of co-catalysts can considerably ameliorate the photocatalytic performance through modulating the d-band centers and providing active sites, including enhanced light absorption, facilitated carrier separation, improved surface catalytic reaction activity, and enhanced photocatalytic stability.

Liu *et al*. modulated the electronic structure of cobalt nitride ($Co_{3.75}N_{0.14}$) by transition metal doping (M = V, Mo, W) to improve its performance in solar-to-hydrogen energy conversion (Fig. 7a).[60] Fig. 7b shows that the doped cobalt-nitride exhibits higher activity in visible light-driven H_2 evolution. In particular, the H_2 evolution rate of V-doped $Co_{3.75}N_{0.14}$ reached 21.21 $\mu mol \cdot mg^{-1} \cdot h^{-1}$ (the highest) under optimal conditions. The results in Fig. 7c indicate that the d-band center position of $Co_{3.75}N_{0.14}$ can be tuned through transition metal doping. DFT calculations showed that the d-band center of the doped cobalt nitride decreased compared with that of the pure cobalt nitride, which facilitated the desorption of hydrogen atoms and thus promoted the hydrogen evolution activity. Zhou *et al*. modulated the d-band center by atomically dispersed transition metal single atoms (TM-SAs, *e.g.*, Co and Ni) on C_3N_4 as well as by P-atom doping to enhance the photocatalytic dechlorination activity.[71] By introducing P atoms, the coordination environments of Co and Ni single atoms can be changed to modulate the location of the d-band center. DFT calculations (Figs. 7d-e) display that the formation of Co/Ni-N_3P_1 coordination site can significantly up-regulate the d-band center to bring it near to the Fermi energy level (EF), which is contributory to charge carriers' transfer. The Gibbs free energy diagram in Fig. 7f displays that the energy of $\cdot O_2^-$ formed at the CCoNiP (carbon nitride containing Co and Ni double single atoms) site is much lower, indicating that the dechlorination process is more likely to occur. The experimental results in Figs. 7g-h show that CCoNiP exhibited excellent performance for the degradation and dechlorination of tetrachlorobisphenol A (TCBPA) underneath visible light irradiation, reaching 100% elimination (44.1% dechlorination with the fastest reaction rate). The principal reason for the above boosted photocatalytic performance is the formation of Co/Ni-N_3P_1 coordination sites in the CCoNiP structure, which contributes to the enhancement of the photogenerated charge carrier transport efficiency and therefore boosts the catalytic activity (Fig. 7i). This study reveals the cooperative effect of P-atom doping and bimetallic single atoms on the d-band centers, which furnishes a novel strategy for devising efficient photocatalysts.[71]

4.1.2 Doping (main catalyst)

Doping of the main catalyst can significantly affect the situation of the d-band center as well as the photocatalytic performance.[52,72-83] Doping can regulate the situation of the d-band center by changing the electronic structure of the catalyst. Doping can also improve the photo-response of the photocatalyst in the visible region, reduce the electron-hole complexation of the surface photogenerated charge, and boost the charge separation efficiency. The d-band center of the main catalyst is regulated through doping, which can achieve good adsorption kinetics and thus improve the redox reaction performance. The photocatalytic performance of the main catalyst can be effectively meliorated through rational doping, which affects multiple steps of the photocatalytic reaction. As an emerging catalyst inside the doped co-catalysts, high-entropy materials are characterized by highly tunable components, which can serve as an excellent platform to explore the catalytic law. The catalysts synthesized through the high-entropy strategy reveal the volcano-shaped relationship between the d-band center of the catalyst and the catalytic activity, and the moderate d-band center can bring the appropriate adsorption strength and the best catalytic effect. In summary, the doping of the main catalyst can optimize the adsorption kinetics and improve the charge separation efficiency and visible light response by regulating the situation of the d-band center, thus significantly enhancing the photocatalytic performance. However, excessive doping may lead to unfavorable structural distortion and charge recombination, reducing the catalytic activity. Therefore, achieving the optimal doping amount and structure is the key to boosting the photocatalytic performance.

Yang *et al*. modulated the electronic structure of bismuth molybdate (Bi_2MoO_6) by cobalt (Co) doping to construct dual active sites and enhance photocatalytic N_2 fixation performance.[84] Through DFT calculations, the researchers found that the upward shift of the d-band center owing to Co doping might be beneficial for physical/chemical adsorption, activation, and hydrogenation of N_2 molecules (Fig. 8a). The experimental results in Fig. 8b show that the prepared 3% Co-Bi_2MoO_6 exhibits the maximum NH_3 output rate of 95.5 $\mu mol \cdot g^{-1} \cdot h^{-1}$ in the absence of a sacrificial agent, which is 7.2 times more excellent that of Bi_2MoO_6. This is imputed to the introduction of Co doping into the impurity energy level, which constructs a dual active site and promotes the carrier separation/conversion kinetics, thus enhancing the photocatalytic nitrogen fixation performance of Bi_2MoO_6. Gong *et al*. modulated the electronic structure of molybdenum

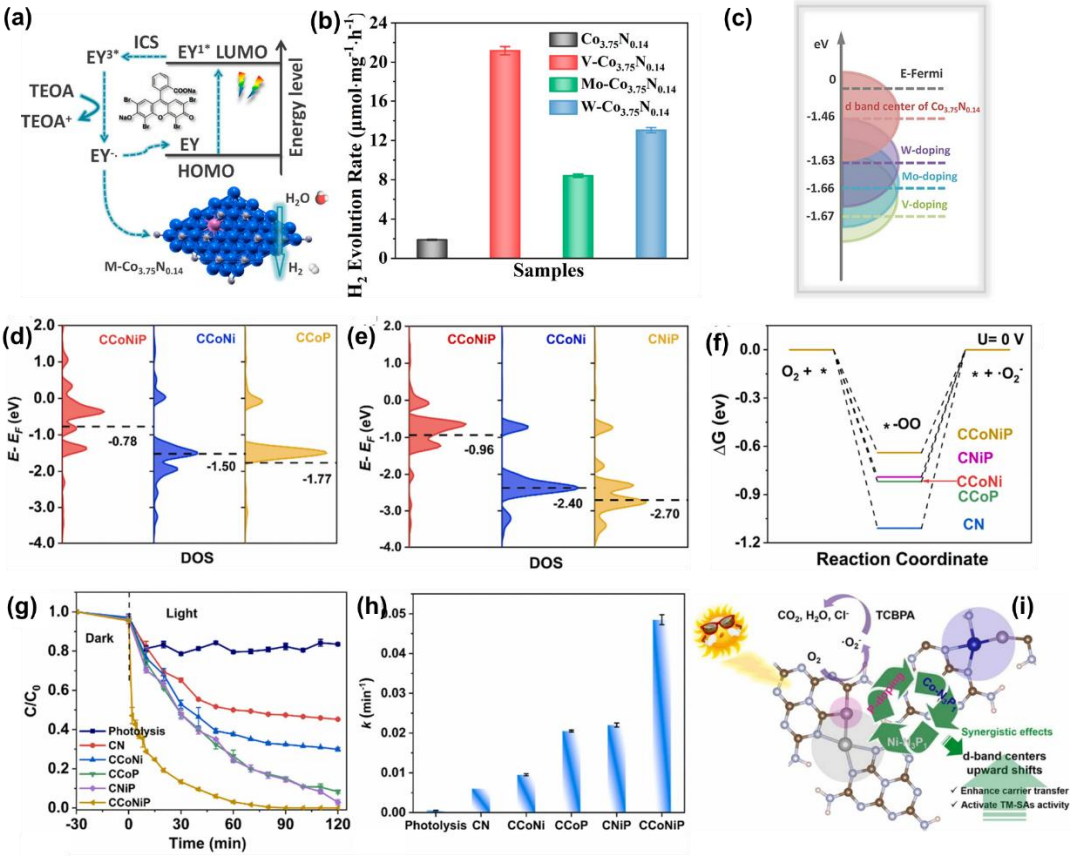

Fig. 7: a) Schematic illustration of conceivable mechanism for the H_2 production in TEOA-EY system for M-$Co_{3.75}N_{0.14}$ catalyst, b) The ordinary rates of H_2 production underneath visible-light (λ > 400 nm) through distinct catalysts in TEOA-EY system, c) d-band center of cocatalysts doped with different elements. a-c reproduced with the permission from [60], Copyright 2023 American Chemical Society. d-e) d-band centers of Co and Ni for the catalysts, f) Gibbs free energy chart of the of the catalysts for $\cdot O_2^-$, * signifies the catalytic sites, g) C/C_0 plots and h) Manifest rate constants of TCBPA over diverse samples underneath visible light irradiation, i) Schematic diagram of reaction mechanism, d-i reproduced with the permission from [71], Copyright 2022 Elsevier.

dicarbide (Mo_2C) by indium (In) doping to enhance its performance in photoreduction of CO_2 to CO in aqueous solution.[85] The experimental results in Figs. 8c-d show that In-doped Mo_2C (In@Mo_2C-d) is capable of reducing CO_2 to CO with 97.3% selectivity at a rate of 234.4 $\mu mol \cdot g^{-1} \cdot h^{-1}$ underneath visible light irradiation. This performance is significantly better than that of undoped Mo_2C. DFT calculations (Figs. 8e-f) show that In doping leads to an upward shift of the d-band center toward the Fermi energy level (Ef), making it easier for electrons to escape and trigger the catalytic reaction. The charge density distinction implies that the electrons are confined to the contiguous Mo sites with local defects, suggesting that In atoms can change the electronic structure of Mo_2C and make the Mo sites electron-rich, thus promoting CO_2 reduction. The enhanced photocatalytic performance of In@Mo_2C-d is imputed to the following: i) In doping introduces a defect energy level, which enhances the separation/transport efficiency of the light-absorbing and photogenerated charge carriers; ii) In doping and defect engineering are capable of enhancing the CO_2 adsorption capacity; iii) In doping lowers the energy barrier of CO_2 reduction reaction and facilitates CO desorption through stabilizing COOH intermediates. The effect of divalent metal cations with distinct d-band centers (M = Mg^{2+}, Ni^{2+}, Cu^{2+}, Zn^{2+}) on the light-driven CO_2 reduction in layered double hydroxides (LDHs) was investigated by Wang *et al.*[51] The experimental results in Figs. 8g-h show that the yields of these LDHs for CO and CH_4 are in the order of MgAl-LDHs < ZnAl-LDHs < CuAl-LDHs < NiAl-LDHs, which suggests that the different electronic structures of the d-bands have a substantial effect on the photocatalytic performance. By varying the species of divalent metal cations, the researchers found that CO_2 activation and electron excitation were more easily achieved when the d-orbitals were partially occupied with active electrons. Valence band XPS (Figs. 8i-j) measurements showed that the d-band center position of NiAl-LDHs and CuAl-LDHs shifted upward, which might be related to their higher activity towards CO_2. The above analysis shows that the d-band center theory furnishes valuable insights in understanding how metal cations modulate the electronic structure of LDHs and their role in photocatalytic CO_2 reduction.

4.1.3 Vacancy/Defect (main catalyst)

The modulation of defects or vacancies in the main catalyst has a significant effect on the d-band center as well as the

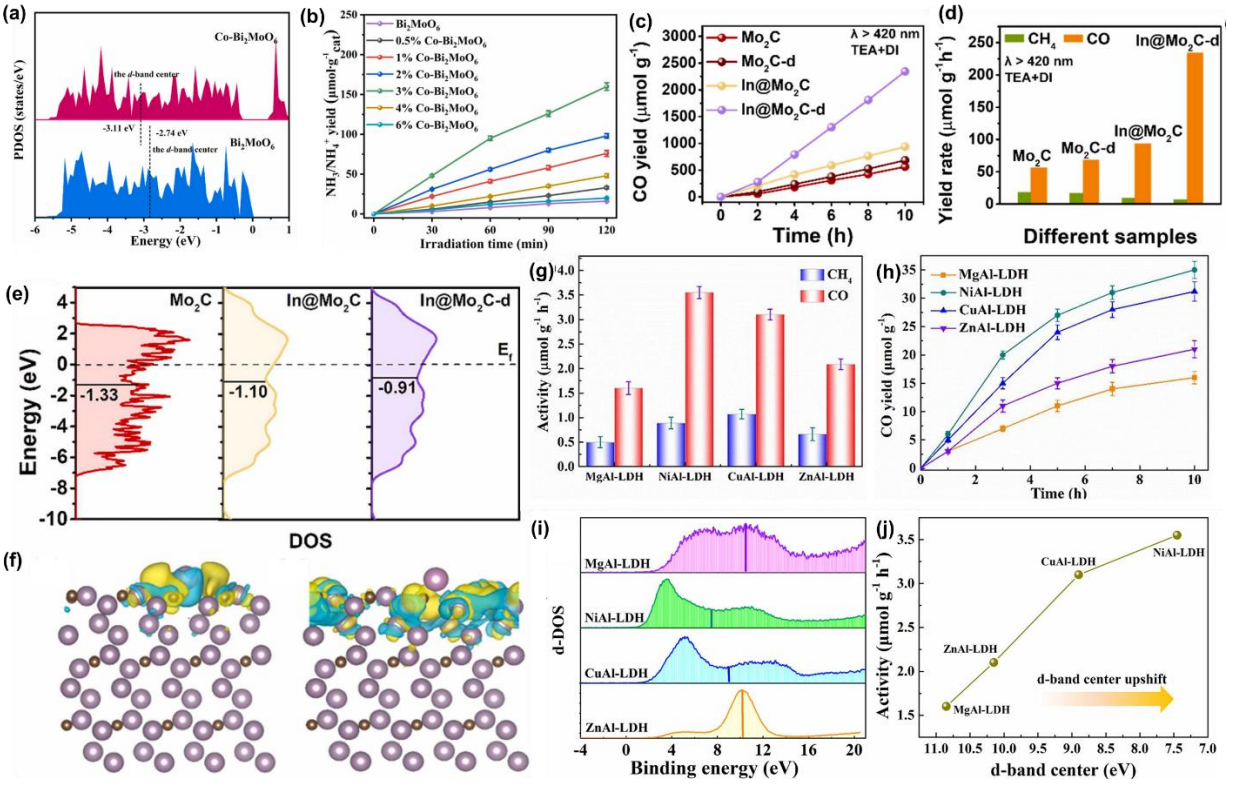

Fig. 8: a) D-band center and PDOS calculation applying the PBE approach of Bi_2MoO_6 and Co-Bi_2MoO_6, b) Photocatalytic N_2 fixation performance of Bi_2MoO_6 and Co-Bi_2MoO_6 underneath visible light, a-b reproduced with the permission from [84], Copyright 2023 Elsevier. c) CO production and d) average gas production rates for CO and CH_4 in aqueous solutions through distinct photocatalysts underneath visible light irradiation at 10 h, e) Total density of states (TDOS) and d-band centers (black line) of Mo_2C, In@Mo_2C and In@Mo_2C-d, f) Crystal constitution of In@Mo_2C (left) and In@Mo_2C-d (right) with differential charge densities (the yellow/blue area stands for the charge's enrichment/loss), c-f reproduced with the permission from [85], Copyright 2022 Elsevier. g) Photocatalytic activity and h) Time-yield plots of LDHs, i) D-band center of the catalysts, j) Relations between activity versus the d-band center situation for LDHs, g-j reproduced with the permission from [51], Copyright 2022 Elsevier.

photocatalytic performance.[86-88] Defects or vacancies can modulate the electronic structure of metal oxides and influence the position of the d-band center (*e.g.*, in the presence of oxygen vacancies, the Fermi energy levels of the oxides move upward, and defect energy levels appear in the band gap, which reduces the width of the energy bands and improves the light absorption performance). Defects or vacancies promote the conversion of excitons into carriers, accelerate surface reactions, and facilitate carrier separation. Defects or vacancies act as active sites and act synergistically with nearby active metal sites to optimize reactant adsorption and improve catalytic activity. Defects or vacancies can regulate the surface characteristics and electronic structure of the photocatalysts without introducing extraneous elements. In summary, the modulation of defects or vacancies in the main catalysts can optimize the position of d-band centers and photocatalytic performance through various mechanisms, including regulating the electronic structure, facilitating carrier separation, providing active sites, and enhancing light absorption and charge migration. These strategies provide novel thoughts for the development of efficient photocatalysts.

Ma *et al*. enhanced the performance of Zn_2GeO_4 nanorods (Mn-ZGO-Vo) in photocatalytic CO_2 reduction to CO by tuning the d-band center.[41] Through DFT calculations, the researchers predicted local lattice distortions and non-uniform charge distributions due to Mn doping and Vo introduction, which led to the rise of the d-band center in Mn-ZGO-Vo (Fig. 9a). Meanwhile, the upward shift of the d-band center of the Mn site relative to the Fermi energy level in the Mn-ZGO-Vo model correlates well with the adsorption energy of CO_2. With the piecemeal upward shift of the d-band center, the CO_2 adsorption strengths were in the order of Mn-ZGO-Vo > Mn-ZGO > ZGO. The experimental results in Fig. 9b showed that the Mn1%-ZGO-Vo catalyst exhibited excellent performance in photoreduction CO_2, with a CO yield of 40.02 $\mu mol \cdot g^{-1} \cdot h^{-1}$, which is virtually eight times more excellent than that of original Zn_2GeO_4. A conceivable photocatalytic mechanism was recommended (Fig. 9c), where Mn doping and the introduction of oxygen vacancies not only increased the number of active sites, but also promoted CO_2 adsorption and activation by upshifting the d-band center. This enhanced interaction contributes to the formation of stable electron transfer channels during the photocatalytic process, which improves the reaction kinetics of CO_2 photoreduction to CO. The effect of constructing bridging oxygen vacancies in $SnTa_2O_6$ nanosheets on improving photocatalytic CO_2

reduction performance was investigated by Zhao *et al.*[89] $SnTa_2O_{6-x}$ showed a 7.5-fold increase in visible light activity over the control sample (pristine $SnTa_2O_6$) after a 40-second flame reduction treatment, exhibiting a higher CO yield (21.1 $\mu mol \cdot g^{-1} \cdot h^{-1}$). This indicates that the introduction of oxygen vacancies significantly boosts the photocatalytic performance (Fig. 9d). By DFT calculations (Fig. 9e), the d-band center of $SnTa_2O_{6-x}$ was positively shifted, which implies that more electrons are distributed around the Fermi energy level, which is favorable for the charge transfer to the adsorbate. This positive shift of the d-band center is associated with the alteration of CO_2 adsorption configuration on $SnTa_2O_{6-x}$. The introduced bridging oxygen vacancies not only upgraded the CO_2 adsorption performance, but also promoted the change of CO_2 activation from monodentate to bidentate adsorption due to the increase of the local charge density and the positive shift of the d-band center, which was favorable for CO_2 adsorption and activation (Fig. 9f).

4.1.4 Heterojunction/homojunction (only between main catalysts)

The modulation of heterojunctions or homojunctions of the main catalysts has a significant effect on the d-band centers as well as the photocatalytic performance.[43,90-94] The constitution of heterojunctions can give rise to the redistribution of electrons, which can adjust the electronic structure of the components and affect the situation of the d-band center. The construction of heterojunctions or homojunctions can improve the photoresponse of the photocatalysts in the visible region, reduce the electron-hole complexation of the surface photogenerated charge, and improve the charge separation efficiency. Specific heterojunction structures exhibit excellent stability, with no decrease in photocurrent and no change in morphology, chemical composition, or structure after prolonged reaction. The heterojunction interface modulation drives the carrier migration mechanism in the direction favorable to the photocatalytic reaction, providing a new

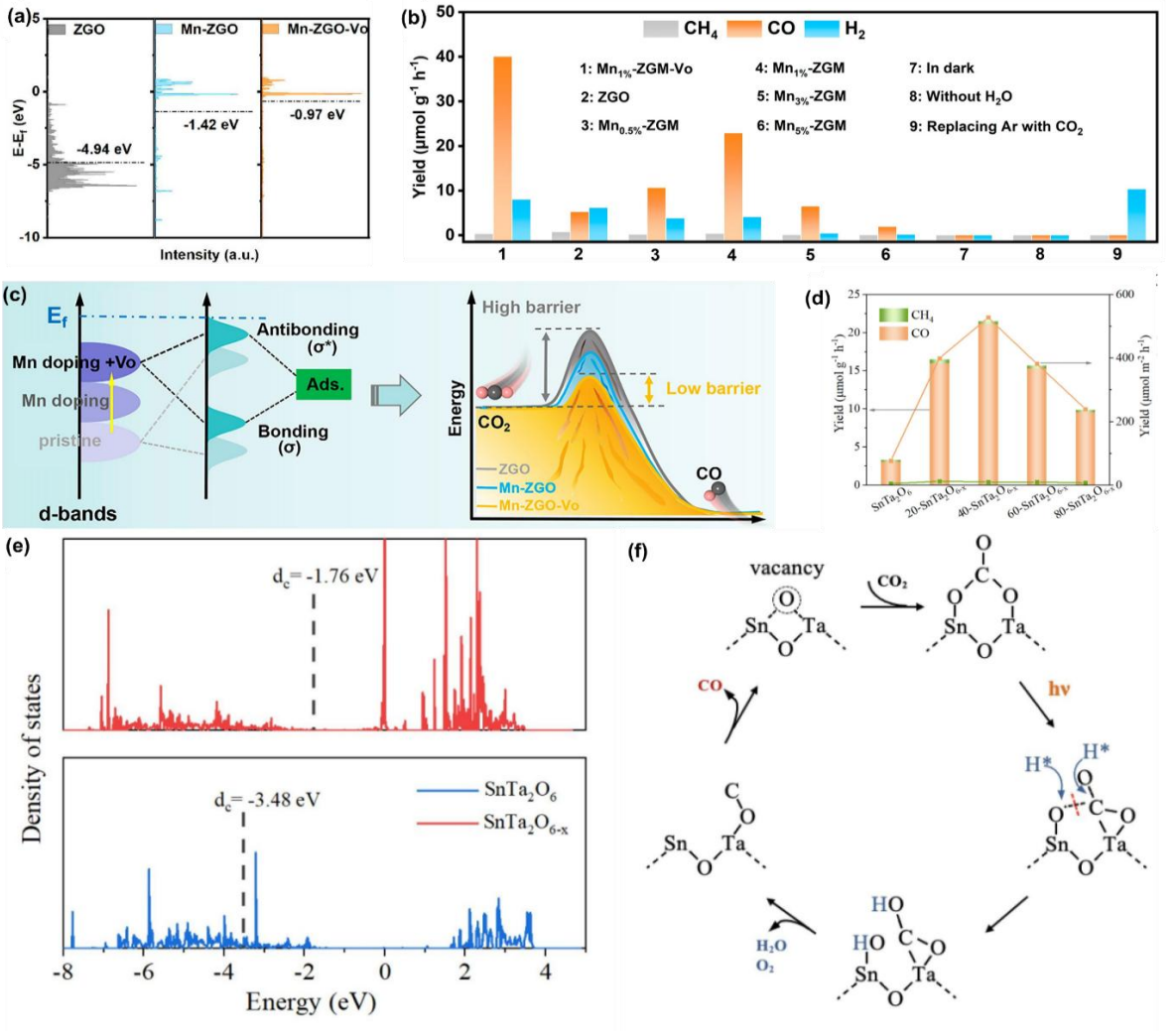

Fig. 9: a) PDOS for Zn/Ge d-orbitals of ZGO and Mn d-orbitals of Mn-ZGO-Vo and Mn-ZGO (the black dash illustrates the d-band center), b) The photoreduction CO_2 performance by means of distinct catalysts, c) Schematic figure of orbital interactions between the adsorbate and the catalysts, diagram of distinct activation energies for Mn-ZGO-Vo, Mn-ZGO, and ZGO, a-c reproduced with the permission from [41], Copyright 2023 Elsevier. d) Photoactivity of $SnTa_2O_6$ and x-$SnTa_2O_{6-x}$ underneath visible light (>400 nm), e) PDOS plots of d bands of Ta, f) Reaction route illustration for CO_2 reduction on $SnTa_2O_{6-x}$, d-f reproduced with the permission from [89], Copyright 2023 Elsevier.

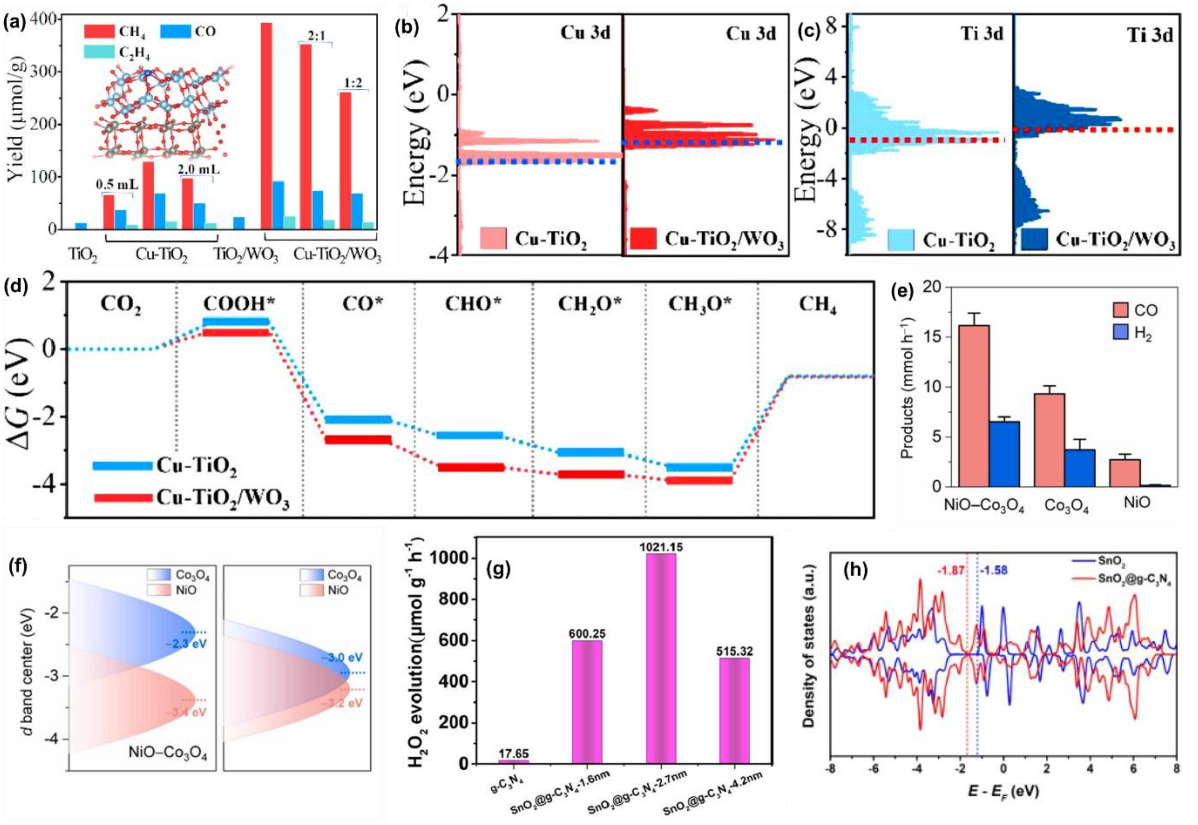

Fig. 10: a) Products from CO_2 photoreduction reaction. The partizan density of states (PDOS) of b) Cu-TiO_2 and c) Cu-TiO_2/WO_3 and the thrown lines symbolize the situations of d-band centers, d) Free-energy charts of CO_2 photoreduction through Cu-TiO_2/WO_3 and Cu-TiO_2 calculated from DFT, a-d reproduced with the permission from [95], Copyright 2024 Elsevier. e) Gas output rate through distinct samples, f) The situation of d-band center of NiO-Co_3O_4, Co_3O_4 and NiO, e-f reproduced with the permission from [96], Copyright 2023 Elsevier. g) H_2O_2 yields of different size of SnO_2 clusters of SnO_2@g-C_3N_4, h) Calculated density of states of original SnO_2 and SnO_2@g-C_3N_4, g-h reproduced with the permission from [61], Copyright 2022 American Chemical Society.

pathway to improve the photocatalytic H_2 production performance of heterojunction catalysts. The catalysts with multiple heterogeneous structures, including crystalline phases, amorphous regions, and heteroatom doping, can improve the catalytic activity of the photocatalysts, which provides a new idea for designing highly efficient photocatalysts. In summary, the modulation of heterojunctions or homojunctions of the main catalysts can optimize the situation of the d-band centers and the photocatalytic performance through various mechanisms, including the adjusting of the electronic constitution, the promotion of carrier separation and transport, and the enhancement of light absorption and utilization efficiency. Zhang *et al*. constructed a Cu single-atom promoted S-scheme heterojunction (Cu-TiO_2/WO_3) for the efficient performance in the photoreduction of CO_2 to CH_4, especially the consequence of upward shift of the d-band centers on the photocatalytic performance.[95] The solar-driven conversion of CO_2 to CH_4 was achieved by the Cu-TiO_2/WO_3 catalysts under the simulated solar irradiation, with a generation rate of 98.69 $\mu mol \cdot g^{-1} \cdot h^{-1}$, and the electron selectivity of CH_4 achieved 88.5%, and this efficiency was much more excellent than that of the TiO_2/WO_3, Cu-TiO_2 and pristine WO_3 (Fig. 10a). By constructing Cu-TiO_2/WO_3 heterojunction, the d-band center positions of Cu and Ti were enhanced (Figs. 10b-c). Further, DFT also calculated the Gibbs free energy change during CO_2 photoreduction and found that the entire process of CO_2 to CH_4 conversion on Cu-TiO_2/WO_3 is thermodynamically more propitious than that on the Cu-TiO_2 surface (Fig. 10d). In particular, the step of forming COOH intermediates is the rate-limiting step for both photocatalysts. The energy required for the formation of COOH intermediates on Cu-TiO_2/WO_3 is 0.54 eV, whereas 0.79 eV is required for Cu-TiO_2, implying that the constitution of Cu-TiO_2/WO_3 can effectively reduce the formation energy of the critical COOH* intermediates. In summary, the upward shift of the d-band center is closely related to the improvement of photocatalytic performance.

Through theoretical calculations and experimental analyses, the researchers revealed the influence of the charge separation effect on the situation of the d-band center in heterojunctions and how these electronic structure changes boost the adsorption, activation, and conversion of CO_2, thus meliorating the performance and selectivity of photoreduction CO_2. Chen *et al*. have developed a device to boost the photoreduction CO_2 performance by constructing NiO-Co_3O_4 ultrathin transverse heterojunctions, especially the effect of the modulation of the d-band centers on the photocatalytic performance.[96] The NiO-Co_3O_4 catalysts have achieved solar-

driven CO_2 to a mixture of CO and H_2 under simulated solar light irradiation conversion, mixing its yield up to 22.67 $mmol \cdot h^{-1}$, and this efficiency was much higher than that of the pristine NiO and Co_3O_4 samples (Fig. 10e). DFT calculations displayed that the electron transfer from NiO to Co_3O_4 led to a rise in the situation of the center of the d-band of Co_3O_4, which boosted the binding strength to the intermediate COOH, which was essential for the photoreduction CO_2 efficiency's enhancement (Fig. 10f). He *et al*. enhanced the photocatalytic performance by anchoring SnO_2 clusters in g-C_3N_4 (SnO_2@g-C_3N_4), especially the relationship between d-band centers and photocatalytic H_2O_2 production underneath visible light irradiation.[61] The experimental consequences proved that SnO_2@g-C_3N_4 achieved efficient photocatalytic H_2O_2 production underneath visible light irradiation with a yield of 1021.15 $\mu mol \cdot g^{-1} \cdot h^{-1}$, which was 58 times more excellent than that of the original g-C_3N_4 (Fig. 10g). DFT calculations displayed that the d-band center of the SnO_2@g-C_3N_4 is reduced owing to the presence of Sn-N bonds, which helps to promote the conversion of OOH to HOOH, a rate-determining step in photocatalytic H_2O_2 production (Fig. 10h).

4.1.5 Heterojunction (between cocatalyst and main catalyst)

Controlling the heterojunction between the primary catalyst (usually a semiconductor material) and the co-catalyst (usually a metal monomer, metal oxide, metal nitride, metal sulfide, metal carbide, or metal phosphide, *etc*.) is critical for optimizing the arrangement of d-band centers and thus influencing the photocatalytic performance.[97-101] By judiciously selecting co-catalysts and tuning their deposition methods, researchers can manipulate the energy band alignment at the heterojunction interface. Correct alignment of the energy levels between the semiconductor conduction band (CB) and the d-band center of the co-catalyst is critical for efficient charge transfer and catalytic activity (*e.g.*, in type II heterojunctions, where the CB of the semiconductor is higher than the d-band center of the co-catalyst, the photogenerated electrons are efficiently transferred to the co-catalyst to facilitate the reduction reaction. On the contrary, in type I heterojunction, the d-band center of the co-catalyst is higher than the CB of the semiconductor, and the charge separation efficiency may be lower, causing lower photocatalytic activity). The presence of the co-catalyst can affect the situation of the d-band center of the semiconductor near the heterojunction interface. The interaction between the semiconductor and the co-catalyst may cause a shift in the d-band center of either material, depending on factors such as energy band bending, charge transfer, and surface chemistry. Proper control of the heterojunction interface can minimize undesirable displacements of the d-band centers, ensure optimal alignment with the reactant energy levels, and maximize photocatalytic activity. The heterojunction interface acts as an active catalytic site for surface reactions, where reactants are adsorbed and photocatalytically transformed. Tuning the morphology, composition and electronic properties of the heterojunction interface can increase the density and accessibility of the catalytic sites, thereby improving the reaction kinetics and overall photocatalytic performance. The loading density and spatial distribution of the co-catalysts on the semiconductor surface affect the charge separation and the catalytic reaction's efficiency. Optimizing the loading and distribution of the co-catalysts ensures adequate coverage of the active sites while minimizing the charge regroupment pathways, thus improving the photocatalytic performance. Apart from facilitating charge transfer, co-catalysts can directly participate in redox reactions by providing adsorption and catalytic active sites. Heterojunction design can promote synergistic interactions between semiconductors and co-catalysts for effective electron transfer and redox mediation, which are crucial for photocatalytic activity. In conclusion, controlling the heterojunction between the main catalyst and the co-catalyst can precisely regulate the d-band center alignment, surface catalytic sites, and charge transfer kinetics, which ultimately affect the photocatalytic performance of the system. Understanding the interplay between semiconductor-co-catalyst interactions and photocatalytic activity is essential for the intellectual design and optimization of heterojunction-based photocatalysts.

Li *et al*. used for the study of photocatalytic hydrogen production performance by constructing CdS/CoS composites.[102] The Gibbs free energy change (ΔGH) of H atom adsorption at distinct sites was investigated by theoretical calculations (Fig. 11a). CdS/CoS exhibited a small ΔGH* value (0.083 eV), indicating its thermodynamically significant hydrogen generation activity. The alterations in the d-band centers of CdS, CoS, and CdS/CoS were further investigated by DFT calculations (Figs. 11b-d), where the formation of Cd-S-Co bonds between CdS nanorods and CoS clusters led to a charge redistribution at the interfaces, which was beneficial for regulating the d-band centers, lowering the thermodynamic energy barriers, and boosting the separation of carriers. The optimized CdS/CoS composite illustrates a superb photocatalytic H_2 generation rate of 65.7 $mmol \cdot g^{-1} \cdot h^{-1}$, which is much more excellent than that of the CdS nanorod photocatalyst (Fig. 11e). This is mainly due to the incremental charge density at the CdS/CoS interface and the improved separation efficiency of photogenerated e^- and h^+. This contributes to the rapid transfer of electrons from the CB of CdS to CoS, which serves as the active site, thus improving the photocatalytic hydrogen production performance (Fig. 11f). Zhang *et al*. constructed NiS/ZnOS (ZnO/ZnS) for photocatalytic hydrogen production performance studies.[103] The NiS-modified ZnOS nanorod heterojunction photocatalysts exhibited excellent photocatalytic hydrogen generation performance with an optimal photocatalytic H_2 production rate of 27 $mmol \cdot g^{-1} \cdot h^{-1}$, which is approximately 7 times more excellent than that of the ZnOS (Fig. 11g). DFT calculations revealed that charge redistribution at the interface formed by ZnO and ZnS helps to regulate the d-band center,

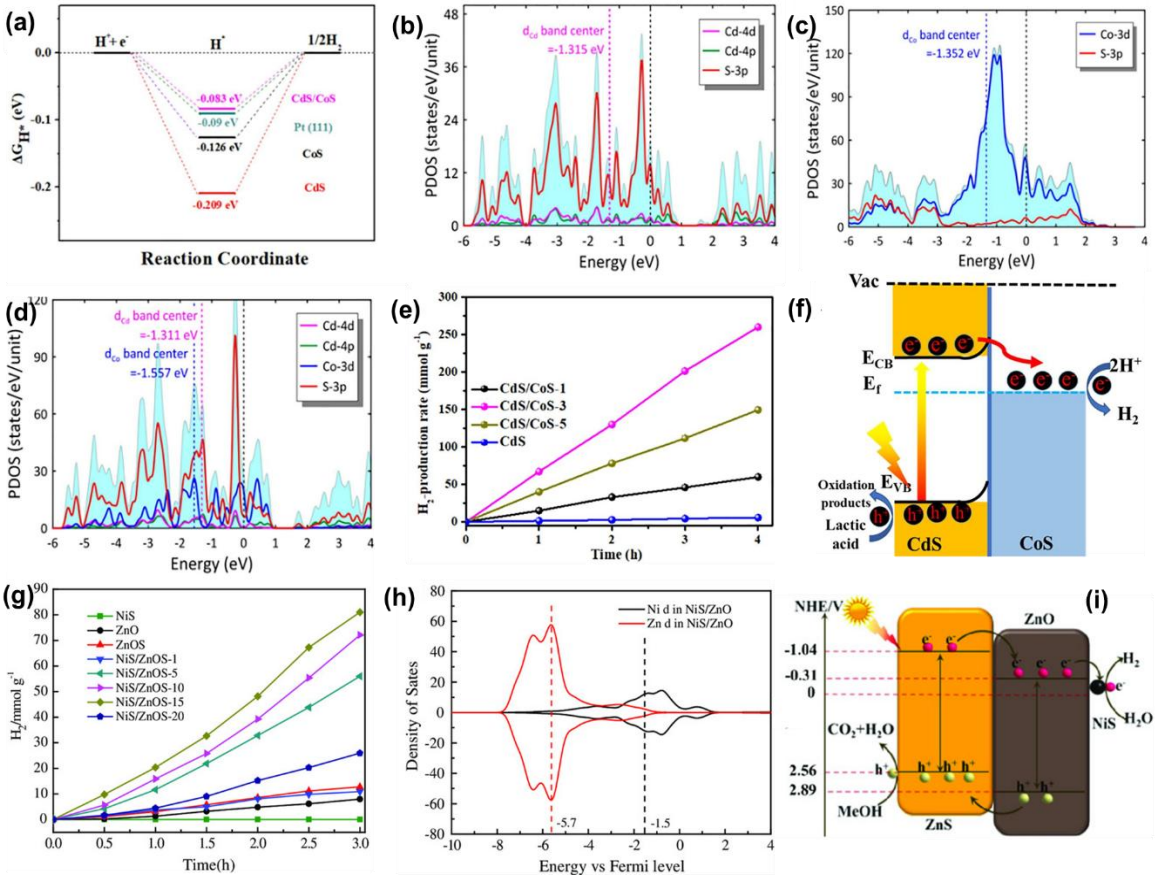

Fig. 11: a) The calculated HER free-energy alteration on CdS/CoS, CoS, and CdS surfaces, b-d) The calculated whole and partial density of state (DOS) and d band center (Cd, Co) of CdS, CoS, and CdS/CoS, e) H_2 output activity over time through the CdS/CoS and CdS, f) Photogenic electron transfer schematic chart, a-f reproduced with the permission from [102], Copyright 2022 Elsevier. g) The line chart of H_2 output rates of NiS/ZnOS-x, h) Projected density of states of the a) NiS/ZnS and b) NiS/ZnO model, i) The conceivable mechanism for the photocatalytic H_2 output over NiS/ZnOS-15 underneath solar light irradiation, g-i reproduced with the permission from [103], Copyright 2020 Wiley.

which affects the photocatalytic performance (Fig. 11h). In the NiS/ZnOS system, the photogenerated electrons can be transferred from the CB of ZnO to NiS faster owing to the modulation of the d-band center, which augments the photogenerated carriers' separation efficiency and thus meliorates the photocatalytic performance (Fig. 11i).

4.1.6 Alloying (co-catalyst)

The alloying modulation of the co-catalysts has a significant consequence on the d-band centers as well as the photocatalytic performance.[104-108] The situation of the d-band center of the metal in the co-catalyst can be changed by alloying, which affects the adsorption capacity for the reaction intermediates. Alloying co-catalysts can provide more active sites and enhance the photogenerated charges' separation efficiency, thus improving the photocatalytic performance. Alloying co-catalysts can optimize the charge separation and transfer efficiency by adjusting the intermetallic electronic structure, decreasing the complexation of photogenerated e^- and h^+, and improving the photocatalytic efficiency. Alloyed co-catalysts usually have better chemical and thermal stability, which helps to boost the stability of the photocatalytic system. Alloying co-catalysts can improve the resistance to toxic substances, which makes it more stable and effective in practical applications. Alloying can produce a synergistic effect in which multiple metal elements work together to optimize the performance of the co-catalysts (*e.g.*, the mechanistic analysis and design of high-entropy alloyed catalysts provide new ideas, emphasizing the importance of moderate d-band centers and adsorption strength). In summary, the alloying modulation of the co-catalysts can optimize the adsorption capacity of the catalysts for reactant molecules and intermediates by influencing the situation of the d-band center, and improve the separation efficiency and stability of photogenerated charges, therefore substantially advancing the photocatalytic performance.

Long *et al*. formed active sites with high selectivity for photocatalytic carbon dioxide (CO_2) conversion to methane (CH_4) through isolating copper (Cu) atoms in the palladium (Pd) lattice.[109] The experimental results in Fig. 12a show that the Pd_7Cu_1-TiO_2 photocatalyst exhibited 96% CH_4 selectivity (19.6 $\mu mol \cdot g_{cat}^{-1} \cdot h^{-1}$) in photoconversion CO_2, which confirms that the photocatalytic performance can be significantly improved through secluding Cu atoms in the Pd lattice. Fig.

12b shows the Cu d band centers calculated by DFT for different Pd_xCu_1 alloy surfaces (*e.g.*, Pd_7Cu_1 and Pd_1Cu_1). The results display that the d-band center of Cu rises when the Cu atoms are encircled through more Pd atoms, which is related to the separation of Cu atoms in the Pd lattice. The rising d-band center contributes to the improvement of the catalytic activity of the Cu sites, which is particularly important for the CO_2 to CH_4 conversion that requires a multi-electron process. In conclusion, through secluding Cu atoms in the Pd lattice, the situation of the d-band centers can be optimized to enhance the adsorption capacity and catalytic activity for CO_2, which is crucial for improving the performance of photocatalytic CO_2 conversion. Theoretical calculations and experimental results together support the rationality of this mechanism. Zhang *et al*. modulated the d-band center by introducing plasmonic monometallic or bimetallic(Au, Ag, Au-Ag) on titanium dioxide (TiO_2) to enhance the photooxidation of 5-hydroxymethylfurfural (5-HMF) to 2,5-furandicarboxylic acid (FDCA).[110] The results in Figs. 12c-d showed that the Ag_1-Au_2/TiO_2 sample had the highest HMF conversion (42.6%) and the highest FDCA selectivity (98.1%), and the highest final FDCA yield (41.8%) was obtained.

As suggested in Fig. 12e, a possible reaction mechanism was proposed in which the plasma metal NPs under visible light irradiation captured light energy and triggered collective oscillations of electrons, generating hot electrons and hot holes. These hot holes can immediately oxidize the HMF molecules adsorbed on the surface of the metal NPs. Meanwhile, the introduction of Au NPs into Ag NPs can regulate the situation of the d-band center to move up to the Fermi Level (Fermi energy level), which affects the reaction intermediates and catalytic performance. In conclusion, the photocatalytic performance can be substantially enhanced through modulating the d-band center and optimizing the band gap structure. The bimetallic Au-Ag/TiO_2 catalyst exhibited excellent performance in the photooxidation of 5-HMF, which was attributed to its ability to separate and transport photogenerated charge carriers more efficiently, as well as to the synergistic effect between Au and Ag nanoparticles. Han *et al*. explored the effect of engineering the d-band center of $AuGa_2$-based plasma nanocomposites on their photocatalytic and antibacterial activities.[111] Fig. 12f demonstrates that the $AuGa_2$/α-Ga_2O_3/Au nanocomposites show significant antimicrobial activity (compared to α-Ga_2O_3) against Staphylococcus aureus (S. aureus) under 808 nm laser irradiation.

The d-band center position of $AuGa_2$ (-4.94 eV) is substantially lower than that of Au (-2.86 eV) is shown in Fig.12g. This decrease in the center of the d-band implies a lower adsorption energy to the intermediate, which may change the reaction pathway and energy potential, and thus the reaction dynamics of the catalytic process. A mechanistic diagram is proposed as in Fig. 12h, where α-Ga_2O_3 generates highly reactive electrons and holes under UV irradiation, which are trapped by O_2 molecules in solution to form superoxide radicals ($\cdot O_2^-$), while the holes react with H_2O molecules to form hydroxyl radicals (·OH). Au and $AuGa_2$ nanoparticles facilitate the transportation and segregation of the charge carriers, and through the plasma effect, enhance the local electric field, generate hot carriers, and increase light absorption. The constitution of heterojunction at the heterogeneous interface of $AuGa_2$ and Au NPs in contact with α-Ga_2O_3 facilitates hot electron transport from $AuGa_2$ and Au NPs to α-Ga_2O_3, and the remaining holes oxidize the H_2O molecules to generate -OH, which is used to kill S. aureus. In summary, the constitution of a heterojunction at the heterogeneous interface of $AuGa_2$ and Au NPs is facilitated by tuning the d-band centers and shapes of $AuGa_2$. The researchers succeeded in improving its photocatalytic performance and achieved enhanced antimicrobial activity against S. aureus under visible light and NIR irradiation. This study demonstrates a new strategy for devising and fabricating bimetallic catalysts with adjustable bandgap structures through d-band engineering and provides a new direction for exploring other liquid metal-based nanocomposites.

4.1.7 Others

In addition to the above mentioned mainstream strategies to modulate the d-band centers of photocatalysts, some other strategies have begun to be focused on, such as coordination environments, single-atom/cluster synergism, metastable metals, and lattice distortion.[53,112-116] Each strategy has its unique advantages and challenges, and usually needs to be selected and optimized according to the specific catalytic system and target reaction. Through the combined application of these strategies, the d-band centers of catalysts can be effectively modulated to improve their performance in diverse catalytic reactions. In the field of photocatalysis, the modulation of the d-band center is especially important for the photocatalytic performance of transition metal catalysts.

4.2 Construction strategy for p-band center

In photocatalysis' field, p-band center's modulation is an important strategy to optimize photocatalysts' electronic structure and thus upgrade their photocatalytic performance. At present, since the p-band center for photocatalytic performance is still relatively small, some modulation strategies have appeared, such as elemental doping, defect modulation, construction of heterostructures, surface modification, and stress engineering.[44,50,66,117-119] Among them, the most applied one is stress engineering, which is mainly due to the fact that the band structure of semiconductors can be altered by applying external stresses or by introducing strains in the material using lattice mismatches. Stress can also cause a displacement of the p-band center, but precise control of the direction and magnitude of the stress is demanded. The second is to construct heterostructures, because heterostructures can efficaciously regulate the p-band center and boost the utilization efficiency of photogenerated carriers. In conclusion, the control strategy of p-band centers in photocatalysis

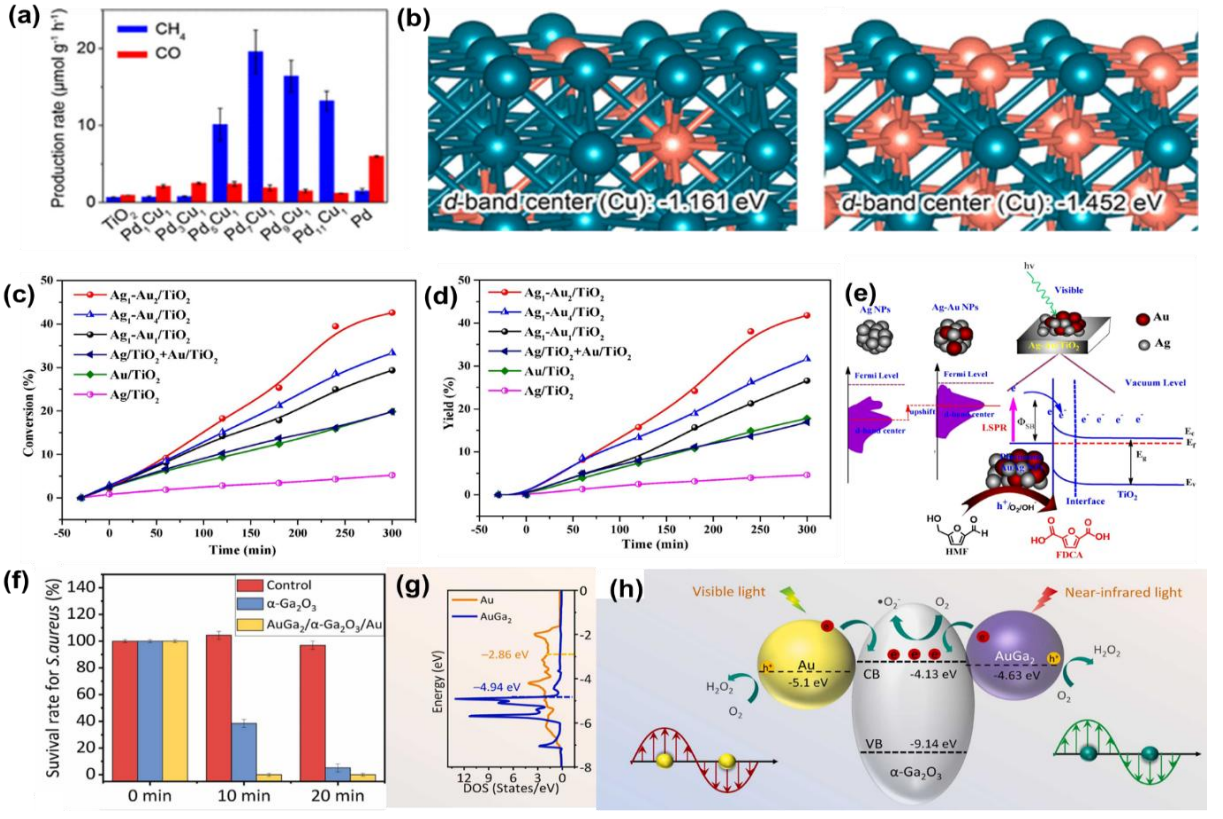

Fig. 12: a) Medial yield rates of CO and CH_4 in photoreduction CO_2 with H_2O through different catalysts, b) The configurable models and Cu d-band centers for ordered Pd_7Cu_1 (left) and (d) Pd_1Cu_1 (right) lattices, a-b reproduced with the permission from [109], Copyright 2017 American Chemical Society. c) Comparison of 5-HMF conversion and d) product (FDCA) yield in the photocatalytic oxidization of HMF through distinct catalysts, e) Schematic diagram of photogenerated charge carriers's constitution process on Au-Ag/TiO_2 underneath visible-light irradiation, c-e reproduced with the permission from [110], Copyright 2023 Elsevier. f) The antibacterial efficiencies' quantitation data determined for the three autonomous experimentations, g) DOS conspiracies of the Au and $AuGa_2$ (d-band center is emphasized in the DOS curve), h) Energy level chart of the $AuGa_2$/α-Ga_2O_3/Au plasmonic composite depicting the conceivable photocatalytic mechanism, f-h reproduced with the permission from [111], Copyright 2023 Elsevier.

involves a series of methods, but the whole is still in the preliminary stage and still needs further exploration. Yue *et al*. explored how the p-band center of bismuth-based metal-organic frameworks (Bi-MOFs) can be modulated by strain engineering in the CO_2 photoreduction reaction and how this modulation affects the photocatalytic performance.[49]

The DFT calculation in Fig.13a shows that the p-band center of the Bi node can be significantly downshifted by applying a huge compressive strain (up to 7.85%) on the Bi-MOF, which enhances the unsaturated state of the Bi node. This downward shift of the p-band center is closely related to the adsorption and activation ability of CO_2 molecules, which has a substantial influence on the efficiency and selectivity of the photoreduction CO_2 reaction. The experimental results in Fig. 13b show that the strain-engineered Bi-MOF/BiOBr composites reached up to 21.95 $\mu mol \cdot g^{-1} \cdot h^{-1}$ CO generation rate and 93% CO_2 to CO selectivity in the absence of a sacrificial agent or co-catalyst. Overall, strain engineering changed the electronic constitution of Bi-MOF, especially the position of the p-band center, which affected the adsorption and activation process of CO_2 molecules, and also favored the desorption process of CO* intermediates, thus boosting the efficiency of the CO_2 photoreduction reaction and the CO selectivity. Zhou *et al*. explored the modulation of $Cs_3Bi_2Br_9$/$BiVO_4$ (s-CBB/HP-BVO) heterojunction by strain engineering to improve its performance in CO_2 photoreduction.[65] DFT calculations in Fig. 13c show that the tensile strain in $Cs_3Bi_2Br_9$ can substantially downshift the p-band center of the active Bi atoms, which upgrades the adsorption/activation of CO_2 by the catalyst. Fig. 13d shows that the s-CBB/HP-BVO composite displays boosted photocatalytic activity under light irradiation with a whole electron expenditure rate of 70.63 $\mu mol \cdot g^{-1} \cdot h^{-1}$ and a CO production selectivity of 79.66%. This work furnishes an in-depth study of the effect of strain engineering on the photocatalytic performance of $Cs_3Bi_2Br_9$/$BiVO_4$ heterojunctions through a combination of experimental and theoretical calculations, especially to optimize the CO_2 adsorption and activation process by modulating the p-band centers, which improves the efficiency and selectivity of photoreduction CO_2. Zhang *et al*. investigated the close relation between the p-band center of S and the photocatalytic mechanism, in particular by constructing Ni@NiS_x-CdS composites for the study of photocatalytic hydrogen

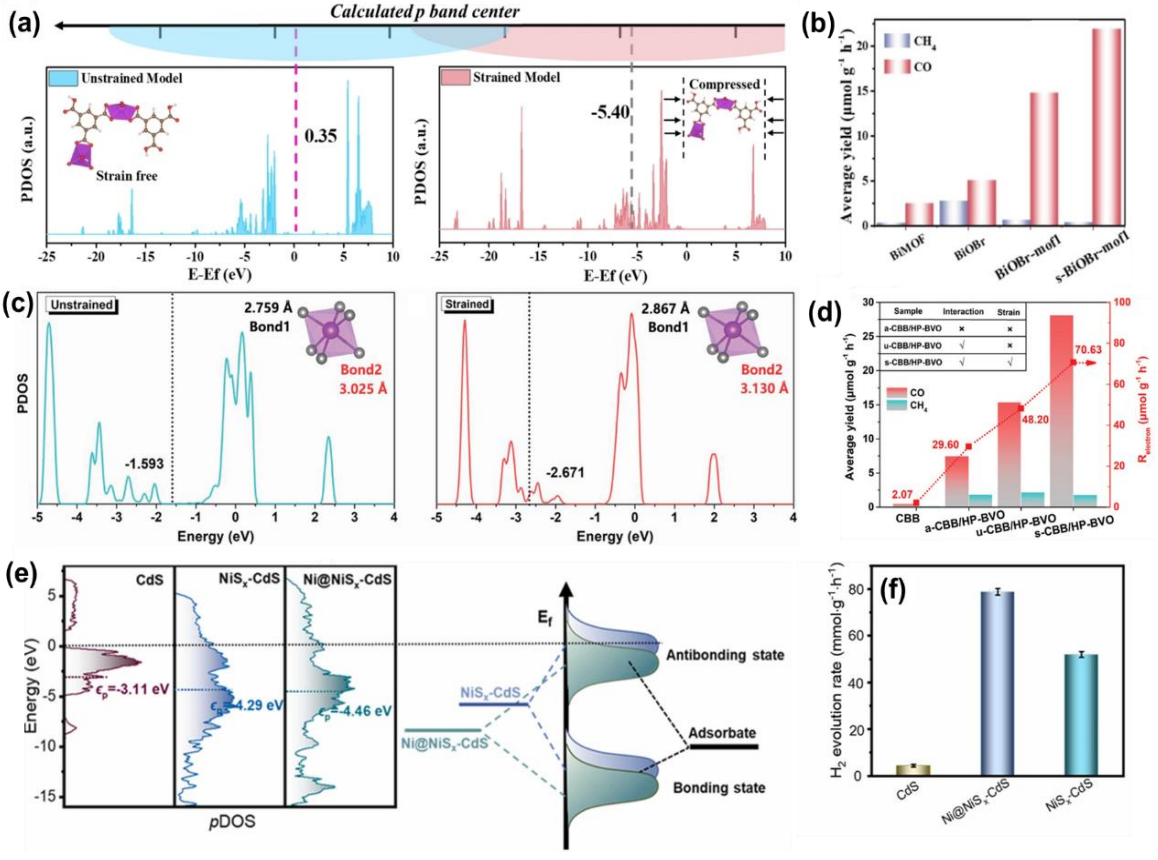

Fig. 13: a) Presented DOS of Bi p and reckoned p band center of as-designed unstrained example and strained example, b) CO and CH_4 yield rates over different photocatalysts, a-b reproduced with the permission from [49], Copyright 2022 Wiley. c) unstrained and strained $Cs_3Bi_2Br_9$ model as well as the relevant crystal formation of [$BiBr_6$] octahedron, d) Gas evolution rate of products on x-CBB/HP-BVO, HP-BVO, and CBB, c-d reproduced with the permission from [65], Copyright 2023 Wiley. e) p-band centers for Ni@NiS_x-CdS, NiS_x-CdS and CdS and the homologous schematic diagram of bond constitution between the adsorbate and the photocatalyst surface, f) Distinct photocatalysts' H_2 development rate, e-f reproduced with the permission from [120], Copyright 2024 Elsevier.

production performance.[120] The positions of the p-band centers of sulfur (S) in the distinct samples were analyzed by theoretical calculations (Fig. 13e). The calculated S p-band centers are located at -3.11 eV (CdS), -4.29 eV (NiS_x-CdS), and -4.46 eV (Ni@NiS_x-CdS), respectively. The further the p-band centers are away from the Fermi energy level, the more the number of anti-bonding states of the H* intermediates are occupied, which leads to the weaker bonding with the active S sites and facilitates the desorption and generation of H_2. The above results indicate that by embedding Ni clusters, Ni@NiS_x-CdS achieves a further downward shift of the p-band center of S, which optimizes the adsorption behavior of H* intermediates and enhances the evolutionary response of H_2. The optimized Ni@NiS_x-CdS photocatalyst exhibited a remarkable photocatalytic hydrogen output rate of 78.7 $mmol \cdot g^{-1} \cdot h^{-1}$ underneath visible light irradiation, which was approximately 1.5 and 18.3 times more excellent than that of NiS_x-CdS and CdS, respectively (Fig. 13f). Through a comprehensive analysis of theoretical calculations and experiments, it was demonstrated that the construction of amorphous Ni@NiS_x co-catalysts not only optimized the electronic structure and p-band center location of CdS, but also enhanced the photogenerated charge extraction and separation efficiency, which gave rise to a substantial amelioration in photocatalytic H_2 generation's performance.

5. Application of d-band center (p-band center) in the field of photocatalysis

As can be seen from Fig. 14, the current control of inner-layer electrons is mainly the d-band center (accounting for about 90%), followed by the p-band center. Regarding the control of the d-band center, the main control is the control of the main catalyst doping, followed by the control of the heterojunction, and then the modulation of the vacancies/defects, with a similar proportion for the other control strategies. These photocatalysts that control the d-band center are mainly used for photocatalytic water splitting (first), CO_2 reduction (second), degradation of organic pollutants (third), N_2 reduction (fourth), *etc*. This is mainly due to the fact that the three previous classes of photocatalytic reactions have some features that are specific to the regulation of d-band centers, which we will describe next.

(1) Tuning the d-band centers in photocatalytic materials offers several advantages for the water decomposition process,

which involves using solar energy to convert water into hydrogen (primarily) and oxygen. Tuning the d-band centers allows for precise alignment of the energy levels between the catalyst and the water molecules. This alignment promotes efficient charge transfer processes, including the generation, separation, and migration of photogenerated e^--h^+ pairs, which are essential for driving the water decomposition reaction. Appropriate adjustment of the d-band center boosts the redox activity of the catalyst, resulting in efficient water oxidation and reduction reactions. Through adjusting the situation of the d-band center, the ability of the catalyst to accept and give electrons during these redox processes can be optimized, thereby increasing the overall water decomposition efficiency. By aligning the d-band center with the energy levels of the water molecule orbitals, the catalyst can selectively adsorb and activate water molecules, boosting water's dissociation into oxygen and hydrogen. The ability to control the d-band center allows the design of photocatalysts according as the specific requirements of water decomposition. By fine-tuning the electronic structure of the catalyst, factors such as energy band alignment, surface chemistry, and reaction kinetics can be optimized to enhance water decomposition activity and selectivity. In conclusion, tuning the d-band center in photocatalytic materials provides multiple advantages for water decomposition, including effective charge transfer, promotion of redox reactions, enhancement of catalytic activity, minimization of charge complexation, synergistic effects with co-catalysts, optimized catalyst design, and utilization of solar energy. These advantages make d-band center modulation a promising strategy for the growth of expeditious and sustainable photocatalysts for the decomposition of water for hydrogen production.

(2) Tuning the d-band center in photocatalytic materials offers several advantages for CO_2 reduction processes, which involve the use of solar energy to transform CO_2 into high value chemicals/fuels. Tuning the d-band center enhances the selective adsorption and activation of CO_2 by precisely aligning the catalyst's energy levels with those of the CO_2 molecule. This alignment facilitates the conversion of CO_2 to target products such as carbon monoxide, methane, or higher hydrocarbons while reducing competing reactions. Additionally, the alignment improves electron transfer kinetics between the catalyst and the CO_2 molecule, driving the CO_2 reduction reaction and promoting an efficient charge transfer process. Catalysts with optimized d-band centers help minimize energy losses, selectively activate CO_2, and promote specific reaction pathways, thereby improving energy efficiency. The ability to control the d-band center allows for the customization of catalysts according to the specific requirements of CO_2 reduction, optimizing reaction selectivity, product distribution, and reaction kinetics, thus enhancing the activity and efficiency of CO_2 reduction. Overall, regulating the d-band center is a promising strategy for rapid and sustainable CO_2 conversion and utilization, offering enhanced selectivity, efficiency, and activity in CO_2 reduction processes.

(3) Tuning the d-band center in photocatalytic materials offers several advantages for contaminant degradation. Tuning the d-band center is crucial for aligning the energetic properties of the catalyst with the target pollutants. This modulation enhances charge transfer efficiency and photocatalytic activity by selectively adsorbing and activating specific pollutants. It also reduces nonspecific interactions and charge carrier recombination, thereby improving overall photocatalytic efficiency. Additionally, optimizing the d-band center contributes to extending the catalyst's lifespan, improving its stability and durability, and providing resistance to surface oxidation, photodegradation, and catalyst poisoning. The ability to control the d-band center allows for tailored catalyst designs suited to specific pollutants and environmental conditions, optimizing photocatalytic performance for various pollutants, including organic dyes, volatile organic compounds (VOCs), and persistent organic pollutants (POPs). Furthermore, photocatalysts with modulated d-band centers have demonstrated positive effects in other photocatalytic reactions such as N_2 reduction, H_2O_2 generation, biomass conversion and antibacterial. Their adjustable energy levels grant them broad application potential across multiple fields.

(4) At present, there are few articles on the modulation of p-band centers for photocatalysts, mainly focusing on the modulation of strain and heterojunction, and their main applications are also mainly focused on photocatalytic hydrogen production and CO_2 reduction. Therefore, the regulation of p-band centers for photocatalysts is still to be further developed and utilized.

6. Conclusion and prospects

In the field of photocatalysis, the concepts of d-band centers and p-band centers are commonly associated with the electronic structure of semiconductor (co-catalyst) photocatalysts, especially in materials such as transition metal sulfides and oxides. d-band centers refer specifically to the energy level positions of the d orbitals of the transition metals, while p-band centers relate to the energy levels of the p orbitals. The positions of these energy levels have important consequences on photocatalysts' performance, including light absorptivity, generation, and separation of e^--h^+ pairs, and catalytic reaction activity. The aim of this review is to furnish a thorough overview of the topic for a diverse audience. The advantages of the d-band (p-band) center strategy are presented, their relevance to the photocatalytic mechanism is explored, and methods for introducing these centers and their applications in various areas of photocatalysis are elucidated. Further, the d-band (p-band) center modulation strategy faces certain challenges and desirable development prospects in the field of photocatalysis.

(1) Designability of catalyst systems: photocatalysts usually involve complex systems containing multiple components, such as semiconductor nanoparticles, metal co-catalysts and surface modifiers. Accurately determining the d-

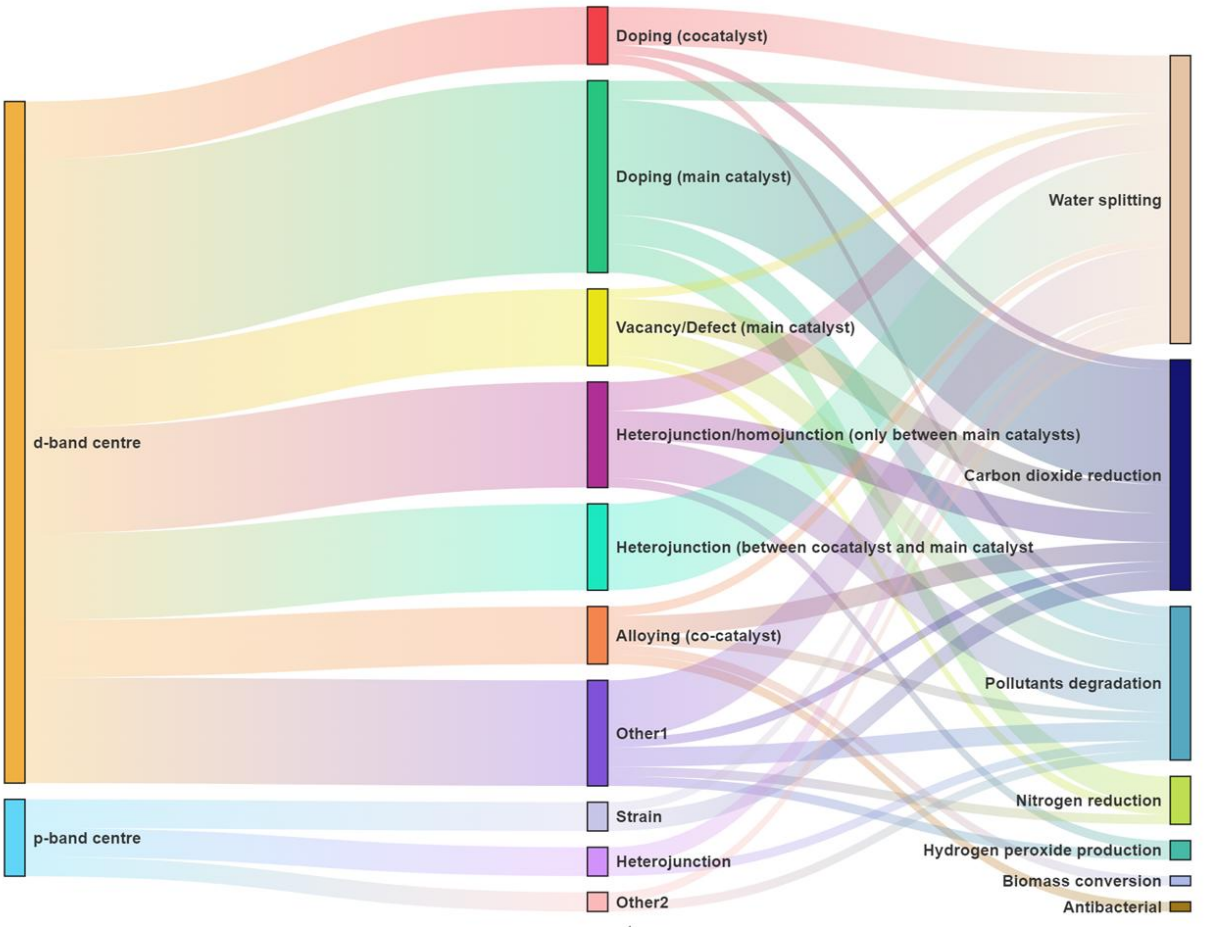

Fig. 14: Distribution of published papers on various modification strategies in photocatalysis applications.

band (p-band) centers of such systems can be challenging due to their complex electronic structures. However, understanding and controlling the d-band (p-band) centers provides the opportunity to tailor the electronic structure of photocatalysts for specific applications. By tuning these parameters, researchers can design photocatalysts with enhanced light absorptivity, charge separation, and reaction dynamics. In addition, current methods for optimizing and tuning the d-band (p-band) centers are relatively simple, and there is a need to develop strategies for better tuning (high entropy, grain boundaries, and π-π interactions, *etc*.).

(2) Improvement of characterization techniques: Continuous improvement of experimental and theoretical characterization techniques allows more precise determination of the d-band (p-band) centers in photocatalytic materials. High-resolution spectroscopic techniques and surface-sensitive probes, among others, contribute to a deeper understanding of electronic structure-activity relationships. Therefore, more sophisticated spectroscopic techniques (*e.g.*, synchrotron-based X-ray spectroscopy and high-resolution electron energy loss spectroscopy (HREELS), *etc*.) are of great importance for exploring the situation of the d-band (p-band) center.

(3) Understanding of the reaction mechanism: Photocatalytic reactions typically occur at the surface of catalyst materials, where interactions with reactants and photoexcited charge carriers take place. d-band (p-band) centers can substantially act on the electronic structure of the catalyst, which in turn influences surface effects and interfacial charge transport. Furthermore, achieving optimal band alignment between the semiconductor and the co-catalyst material is essential for efficacious charge separation and photocatalytic performance. Accurate control of the situations of the d-band (p-band) centers to achieve favorable band alignment remains a challenge. Therefore, in-situ characterizations that can show the locations of the d-band (p-band) centers need to be explored in depth in order to access a more precise analysis of the reaction sites and the reaction mechanism.

(4) Importance of DFT and machine learning: Machine learning algorithms can be trained on the data from DFT calculations to develop predictive models for estimating the d-band (p-band) centers of catalyst materials. These models can capture the complex relationship between material properties and electronic structure, enabling rapid screening of candidate materials for catalytic applications. Integrating machine learning predictions with experimental validation can enhance the reliability and applicability of computational models in guiding catalyst design and optimization efforts. In summary, the relationship between d-band (p-band) centers, DFT, and machine learning involves the use of computational and data-driven approaches to understand and predict the electronic

structure of catalyst materials. Combining DFT calculations with machine learning techniques offers the opportunity to accelerate material discovery and design for catalytic applications while addressing key challenges in accuracy, interpretability, and validation.

(5) Exportability of emerging materials: The development of novel photocatalytic materials and nanostructures provides new opportunities to exploit the concept of d-band (p-band) centers. Tailoring the electronic properties of nanomaterials through size, shape, and composition control can fine-tune photocatalytic performance. While challenges remain in accurately identifying and controlling the d-band (p-band) centers of photocatalytic materials, their application offers significant promise for advancing the field towards more efficient and sustainable environmental remediation and energy conversion technologies. In addition, the impact of modulation with deeper inner electrons (f-band centers) on the catalytic performance of semiconductors can be explored.

(6) Practical application: The practical application of the d-band (p-band) center in the industrial field has moved from the laboratory to large-scale production, and has become the core means to promote the landing of green technology. Suitable catalyst materials can be selected according to the d-band (p-band) center theory in industrial processes such as photocatalytic hydrogen production by water decomposition, CO_2 reduction, and pollutant degradation. At the same time, the d-band (p-band) center is regulated by doping, constructing heterojunction and other technological means, the electronic structure of the catalyst is accurately regulated, and the existing catalyst is optimized or the novel catalyst is designed to increase its catalytic performance and improve the industrial production efficiency, which provides an effective way for the photocatalysis to industrial practical application.

Acknowledgments

This study was financially supported by the Natural Sciences and Engineering Research Council of Canada-Discovery Grant (Canada), the Key project of National Natural Science Foundation of China (NO. 32430071 and 32071713).

Conflict of Interest

There is no conflict of interest.

Supporting Information

Not applicable.

References

[1] J. Brodny, M. Tutak, Decade of Progress: A multidimensional measurement and assessment of energy sustainability in EU-27 nations, *Applied Energy*, 2025, **382**, 125222, doi: 10.1016/j.apenergy.2024.125222.

[2] J. Brodny, M. Tutak, Analysis of the diversity in emissions of selected gaseous and particulate pollutants in the European Union countries, *Journal of Environmental Management*, 2019, **231**, 582-595, doi: 10.1016/j.jenvman.2018.10.045.

[3] N. C. Chiu, J. M. Lessard, E. N. Musa, L. S. Lancaster, C. Wheeler, T. D. Krueger, C. Chen, T. C. Gallagher, M. T. Nord, H. Huang, P. H. Cheong, C. Fang, K. C. Stylianou, Elucidation of the role of metals in the adsorption and photodegradation of herbicides by metal-organic frameworks, *Nature Communications*, 2024, **15**, 1459, doi: 10.1038/s41467-024-45546-y.

[4] L. Lin, Y. Ma, J. J. M. Vequizo, M. Nakabayashi, C. Gu, X. Tao, H. Yoshida, Y. Pihosh, Y. Nishina, A. Yamakata, N. Shibata, T. Hisatomi, T. Takata, K. Domen, Efficient and stable visible-light-driven Z-scheme overall water splitting using an oxysulfide H_2 evolution photocatalyst, *Nature Communications*, 2024, **15**, 397, doi: 10.1038/s41467-024-44706-4.

[5] M. Khater, P. Yeole, S. Khater, H. Gholap, Photocatalytic degradation of antibiotics by titanium dioxide (TiO_2) nanoparticles, *ES Energy & Environment*, 2024, **26**, 1277, doi: 10.30919/esee1277.

[6] V. Kadam, C. Jagtap, V. Kumkale, U. Rednam, P. Lokhande, H. Pathan, Photocatalytic degradation of rose Bengal dye using chemically synthesized pristine and molybdenum doped zinc oxide, *Engineered Science*, 2024, **28**, 1077, doi: 10.30919/es1077.

[7] C. Lin, Y. Zhang, S. Zhang, X. X. Wang, J. Yang, J. Li, X. Lu, B. Liu, Facile fabrication of a novel g-C_3N_4/CdS composites catalysts with enhanced photocatalytic performances, *ES Energy & Environment*, 2023, **20**, 860, doi: 10.30919/esee8c860.

[8] T. Serikov, E. Seliverstova, A. Sadykova, N. Ibrayev, N. Nuraje, Size effect of gold nanoparticles on the photocatalytic activity of titanium dioxide/reduced graphene oxide (TiO_2/rGO) nanocomposite, *Engineered Science*, 2024, **32**, 1327, doi: 10.30919/es1327.

[9] S. Li, C. You, F. Yang, G. Liang, C. Zhuang, X. Li, Interfacial Mo-S bond modulated S-scheme $Mn_{0.5}Cd_{0.5}S/Bi_2MoO_6$ heterojunction for boosted photocatalytic removal of emerging organic contaminants, *Chinese Journal of Catalysis*, 2025, **68**, 259-271, doi: 10.1016/S1872-2067(24)60181-6.

[10] S. Li, K. Rong, X. Wang, C. Shen, F. Yang, Q. Zhang, Design of carbon quantum dots/CdS/Ta_3N_5 S-scheme heterojunction nanofibers for efficient photocatalytic antibiotic removal, *Acta Physico-Chimica Sinica*, 2024, **40**, 2403005, doi: 10.3866/PKU.WHXB202403005.

[11] D. Xie, Y. Kuang, B. Yuan, Y. Zhang, C. Ye, Y. Guo, H. Qiu, J. Ren, S. O. Alshammari, Q. A. Alshammari, Z. M. El-Bahy, K. Zhao, Z. Guo, Q. Rao, S. Yang, Convenient and

highly efficient adsorption of diosmetin from lemon peel by magnetic surface molecularly imprinted polymers, *Journal of Materials Science & Technology*, 2025, **211**, 159-170, doi: 10.1016/j.jmst.2024.06.001.

[12] C. W. Tsao, S. Narra, J. Kao, Y. Lin, C. Chen, Y. Chin, Z. Huang, W. Huang, C. Huang, C. Luo, J. Chou, S. Ogata, M. Sone, M. Huang, T. Chang, Y. Lo, Y. Lin, E. W. Diau, Y. J. Hsu, Dual-plasmonic Au@Cu_7S_4 yolk@shell nanocrystals for photocatalytic hydrogen production across visible to near infrared spectral region, *Nature Communications*, 2024, **15**, 413, doi: 10.1038/s41467-023-44664-3.

[13] Y. Guo, B. Zhu, C. Y. Tang, Q. Zhou, Y. Zhu, Photogenerated outer electric field induced electrophoresis of organic nanocrystals for effective solid-solid photocatalysis, *Nature Communications*, 2024, **15**, 428, doi: 10.1038/s41467-024-44700-w.

[14] Y. Guan, H. Wen, K. Cui, Q. Wang, W. Gao, Y. Cai, Z. Cheng, Q. Pei, Z. Li, H. Cao, T. He, J. Guo, P. Chen, Light-driven ammonia synthesis under mild conditions using lithium hydride, *Nature Chemistry*, 2024, **16**, 373-379, doi: 10.1038/s41557-023-01395-8.

[15] X. Chen, J. Zhao, G. Li, D. Zhang, H. Li, Recent advances in photocatalytic renewable energy production, *Energy Materials*, 2022, **2**, 2000001, doi: 10.20517/energymater.2021.24.

[16] H. Liu, N. Yan, H. Bai, R. T. K. Kwok, B. Z. Tang, Aggregation-induced emission luminogens for augmented photosynthesis, *Exploration*, 2022, **2**, 20210053, doi: 10.1002/EXP.20210053.

[17] J. Ning, B. Zhang, L. Siqin, G. Liu, Q. Wu, S. Xue, T. Shao, F. Zhang, W. Zhang, X. Liu, Designing advanced S-scheme CdS QDs/La-Bi_2WO_6 photocatalysts for efficient degradation of RhB, *Exploration*, 2023, **3**, 20230050, doi: 10.1002/EXP.20230050.

[18] W. Cao, W. Zhang, L. Dong, Z. Ma, J. Xu, X. Gu, Z. Chen, Progress on quantum dot photocatalysts for biomass valorization, *Exploration*, 2023, **3**, 20220169, doi: 10.1002/exp.20220169.

[19] C. You, C. Wang, M. Cai, Y. Liu, B. Zhu, S. Li, Improved photo-carrier transfer by an internal electric field in BiOBr/nrich C_3N_5 3D/2D S-scheme heterojunction for efficiently photocatalytic micropollutant removal, *Acta Physico-Chimica Sinica*, 2024, **40**, 2407014, doi: 10.3866/PKU.WHXB202407014.

[20] C. Wang, C. You, K. Rong, C. Shen, F. Yang, S. Li, An S-scheme MIL-101(Fe)-on-BiOCl heterostructure with oxygen vacancies for boosting photocatalytic removal of Cr(VI), *Acta Physico-Chimica Sinica*, 2024, **40**, 2307045, doi: 10.3866/PKU.WHXB202307045.

[21] S. Li, K. Dong, M. Cai, X. Li, X. Chen, A plasmonic S-scheme Au/MIL-101(Fe)/BiOBr photocatalyst for efficient synchronous decontamination of Cr(VI) and norfloxacin antibiotic, *eScience*, 2024, **4**, 100208, doi: 10.1016/j.esci.2023.100208.

[22] P. Wang, X. Zhang, R. Shi, J. Zhao, G. I. N. Waterhouse, J. Tang, T. Zhang, Photocatalytic ethylene production by oxidative dehydrogenation of ethane with dioxygen on ZnO-supported PdZn intermetallic nanoparticles, *Nature Communications*, 2024, **15**, 789, doi: 10.1038/s41467-024-45031-6.

[23] J. Wang, K. Song, T. Luan, K. Cheng, Q. Wang, Y. Wang, W. W. Yu, P. Li, Y. Zhao, Robust links in photoactive covalent organic frameworks enable effective photocatalytic reactions under harsh conditions, *Nature Communications*, 2024, **15**, 1267, doi: 10.1038/s41467-024-45457-y.

[24] A. Q. Malik, H. Singh, A. Kumar, R. Aepuru, D. Kumar, T. U. G. Mir, Q. U. Ain, A. Ahmad Bhat, A. Mubayi, An overview on magnetic separable spinel as a promising materials for photocatalysis and waste water treatment, *ES Energy & Environment*, 2022, **19**, 744, doi: 10.30919/esee8c744.

[25] S. Chen, L. Zhang, D. A. Alshammari, M. M. Hessien, W. Yu, L. Cui, J. Ren, Z. M. El-Bahy, Z. Guo, Z-scheme Ag_2O/ZnO heterostructure on carbon fibers for efficient photocatalysis of tetracycline, *Separation and Purification Technology*, 2025, **354**, 129414, doi: 10.1016/j.seppur.2024.129414.

[26] X. Xin, Y. Li, Y. Zhang, Y. Wang, X. Chi, Y. Wei, C. Diao, J. Su, R. Wang, P. Guo, J. Yu, J. Zhang, A. J. Sobrido, M. M. Titirici, X. Li, Large electronegativity differences between adjacent atomic sites activate and stabilize $ZnIn_2S_4$ for efficient photocatalytic overall water splitting, *Nature Communications*, 2024, **15**, 337, doi: 10.1038/s41467-024-44725-1.

[27] M. H. Elsayed, M. Abdellah, A. Z. Alhakemy, I. M. A. Mekhemer, A. E. A. Aboubakr, B. Chen, A. Sabbah, K. Lin, W. Chiu, S. Lin, C. Chu, C. Lu, S. Yang, M. Mohamed, S. Kuo, C. Hung, L. Chen, K. Chen, H. Chou, Overcoming small-bandgap charge recombination in visible and NIR-light-driven hydrogen evolution by engineering the polymer photocatalyst structure, *Nature Communications*, 2024, **15**, 707, doi: 10.1038/s41467-024-45085-6.

[28] R. Liu, Y. Chen, H. Yu, M. Položij, Y. Guo, T. C. Sum, T. Heine, D. Jiang, Linkage-engineered donor-acceptor covalent organic frameworks for optimal photosynthesis of hydrogen peroxide from water and air, *Nature Catalysis*, 2024, **7**, 195-206, doi: 10.1038/s41929-023-01102-3.

[29] S. S. Wagh, A. C. S. I. SGVPM's A, D. B. Salunkhe, S. P.

Patole, S. Jadkar, R. S. Patil, A. C. S. I. GVPM's A, Zinc oxide decorated carbon nanotubes composites for photocatalysis and antifungal application, *ES Energy & Environment*, 2023, **21**, 945, doi: 10.30919/esee945.

[30] B. Wang, G. Chen, B. Hu, L. Chen, X. Wang, S. Tian, X. Hu, Y. Li, C. Peng, S. Yin, Recent advances in tunable metal-support interactions for enhancing the photocatalytic nitrogen reduction reaction, *EES Catalysis*, 2024, **2**, 180-201, doi: 10.1039/D3EY00191A.

[31] J. Hu, F. Yang, J. Qu, Y. Cai, X. Yang, C. M. Li, Synergetic bimetallic catalysts: A remarkable platform for efficient conversion of CO_2 to high value-added chemicals, *Journal of Energy Chemistry*, 2023, **87**, 162-191, doi: 10.1016/j.jechem.2023.08.009.

[32] D. Banerjee, N. Kushwaha, N. P. Shetti, T. M. Aminabhavi, E. Ahmad, Green hydrogen production *via* photo-reforming of bio-renewable resources, *Renewable and Sustainable Energy Reviews*, 2022, **167**, 112827, doi: 10.1016/j.rser.2022.112827.

[33] Y. Xin, S. Li, Y. Qian, W. Zhu, H. Yuan, P. Jiang, R. Guo, L. Wang, High-entropy alloys as a platform for catalysis: progress, challenges, and opportunities, *ACS Catalysis*, 2020, **10**, 11280-11306, doi: 10.1021/acscatal.0c03617.

[34] X. Wang, G. Zhang, L. Yang, E. Sharman, J. Jiang, Material descriptors for photocatalyst/catalyst design, *WIREs Computational Molecular Science*, 2018, **8**, e1369, doi: 10.1002/wcms.1369.

[35] X. Cui, J. Wang, B. Liu, S. Ling, R. Long, Y. Xiong, Turning Au nanoclusters catalytically active for visible-light-driven CO_2 reduction through bridging ligands, *Journal of the American Chemical Society*, 2018, **140**, 16514-16520, doi: 10.1021/jacs.8b06723.

[36] C. Yang, N. Balakrishnan, V. R. Bhethanabotla, B. Joseph, Interplay between subnanometer Ag and Pt clusters and anatase TiO_2 (101) surface: implications for catalysis and photocatalysis, *The Journal of Physical Chemistry C*, 2014, **118**, 4702-4714, doi: 10.1021/jp4112525.

[37] Y. Wang, S. Jiang, C. Sun, S. Song, Synchronously regulating d- and p-band centers of heterojunction photocatalysts by strain effect for solar energy conversion into H_2, *Journal of Materials Science & Technology*, 2024, **190**, 210-217, doi: 10.1016/j.jmst.2023.12.026.

[38] S. Sun, X. Zhou, B. Cong, W. Hong, G. Chen, Tailoring the d-band centers endows $(Ni_xFe_{1-x})_2P$ nanosheets with efficient oxygen evolution catalysis, *ACS Catalysis*, 2020, **10**, 9086-9097, doi: 10.1021/acscatal.0c01273.

[39] R. Zeng, Q. Gao, L. Xiao, W. Wang, Y. Gu, H. Huang, Y. Tan, D. Tang, S. Guo, Precise tuning of the D-band center of dual-atomic enzymes for catalytic therapy, *Journal of the American Chemical Society*, 2024, **146**, 10023-10031, doi: 10.1021/jacs.4c00791.

[40] Z. Hou, C. Cui, Y. Li, Y. Gao, D. Zhu, Y. Gu, G. Pan, Y. Zhu, T. Zhang, Lattice-strain engineering for heterogenous electrocatalytic oxygen evolution reaction, *Advanced Materials*, 2023, **35**, 2209876, doi: 10.1002/adma.202209876.

[41] Z. Ma, X. Liu, X. Wang, Z. Luo, W. Li, Y. Nie, L. Pei, Q. Mao, X. Wen, J. Zhong, Manipulating the d-band center enhances photoreduction of CO_2 to CO in Zn_2GeO_4 nanorods, *Chemical Engineering Journal*, 2023, **468**, 143569, doi: 10.1016/j.cej.2023.143569.

[42] X. Sun, L. Sun, G. Li, Y. Tuo, C. Ye, J. Yang, J. Low, X. Yu, J. H. Bitter, Y. Lei, D. Wang, Y. Li, Phosphorus tailors the*d*-band center of copper atomic sites for efficient CO_2 photoreduction under visible-light irradiation, *Angewandte Chemie International Edition*, 2022, **61**, e202207677, doi: 10.1002/anie.202207677.

[43] B. Zhao, X. Long, Q. Zhao, M. Shakouri, R. Feng, L. Lin, Y. Zeng, Y. Zhang, X. Fu, J. Luo, *In situ* self-heterogenization of Cu_2S/CuS nanostructures with modulated d band centers for promoting photocatalytic degradation and hydrogen evolution performances, *Materials Today Nano*, 2023, **23**, 100362, doi: 10.1016/j.mtnano.2023.100362.

[44] F. Wu, X. Zhang, L. Wang, G. Li, J. Huang, A. Song, A. Meng, Z. Li, Enhanced spin-polarized electric field modulating p-band center on Ni-doped CdS for boosting photocatalytic hydrogen evolution, *Small*, 2024, **20**, e2309439, doi: 10.1002/smll.202309439.

[45] T. Guo, H. Fei, R. Liu, F. Liu, D. Wang, Z. Wu, Constructing molybdenum vacancy defect for MoP with optimized p-band center towards high-efficiency hydrogen evolution, *Applied Catalysis B: Environmental*, 2024, **343**, 123480, doi: 10.1016/j.apcatb.2023.123480.

[46] P. Zhou, M. Luo, S. Guo, Optimizing the semiconductor-metal-single-atom interaction for photocatalytic reactivity, *Nature Reviews Chemistry*, 2022, **6**, 823-838, doi: 10.1038/s41570-022-00434-1.

[47] S. Zhou, W. Pei, Y. Zhao, X. Yang, N. Liu, J. Zhao, Low-dimensional non-metal catalysts: principles for regulating p-orbital-dominated reactivity, *NPJ Computational Materials*, 2021, **7**, 186, doi: 10.1038/s41524-021-00654-x.

[48] J. Zhang, W. Li, J. Wang, X. Pu, G. Zhang, S. Wang, N. Wang, X. Li, Engineering p-band center of oxygen boosting H^+ intercalation in δ-MnO_2 for aqueous zinc ion batteries, *Angewandte Chemie International Edition*, 2023, **62**, e202215654, doi: 10.1002/anie.202215654.

[49] X. Yue, L. Cheng, F. Li, J. Fan, Q. Xiang, Highly strained Bi-MOF on bismuth oxyhalide support with tailored intermediate adsorption/desorption capability for robust CO_2

photoreduction, *Angewandte Chemie International Edition*, 2022, **61**, e202208414, doi: 10.1002/anie.202208414.
[50] D. Gao, P. Deng, J. Zhang, L. Zhang, X. Wang, H. Yu, J. Yu, Reversing free-electron transfer of MoS_{2+x} cocatalyst for optimizing antibonding-orbital occupancy enables high photocatalytic H_2 evolution, *Angewandte Chemie International Edition*, 2023, **62**, e202304559, doi: 10.1002/anie.202304559.
[51] R. Wang, Z. Qiu, S. Wan, Y. Wang, Q. Liu, J. Ding, Q. Zhong, Insight into mechanism of divalent metal cations with different d-bands classification in layered double hydroxides for light-driven CO_2 reduction, *Chemical Engineering Journal*, 2022, **427**, 130863, doi: 10.1016/j.cej.2021.130863.
[52] H. Wu, J. Peng, H. Sun, Q. Ruan, H. Dong, Y. Jin, Z. Sun, Y. Hu, Surface activation of calcium tungstate by europium doping for improving photocatalytic performance: Towards lanthanide site photocatalysis, *Chemical Engineering Journal*, 2022, **432**, 134339, doi: 10.1016/j.cej.2021.134339.
[53] F. Wu, Y. Dou, J. Zhou, J. Qin, T. Jiang, Y. Yao, C. Hélix-Nielsen, W. Zhang, High-entropy $(FeCoNiCuZn)WO_4$ photocatalysts-based fibrous membrane for efficient capturing and upcycling of plastic, *Chemical Engineering Journal*, 2023, **470**, 144134, doi: 10.1016/j.cej.2023.144134.
[54] X. Tao, J. Ren, D. Wang, H. Huang, Y. Li, D. Guo, B. Shan, Y. Liu, J. Wang, Y. Zhen, Z. Niu, Refining the d-band center of S-scheme $CdIn_2S_4/MnZnFe_2O_4$ heterostructures by interfacial electric field with boosting photocatalytic performance, *Chemical Engineering Journal*, 2023, **478**, 147347, doi: 10.1016/j.cej.2023.147347.
[55] Z. Liu, Y. Tian, S. Yao, Y. Li, Y. Fu, Q. Zhou, Interfacial interaction-induced shift of d-band center promotes photocatalytic antibiotics mineralization, *Applied Catalysis B: Environment and Energy*, 2024, **352**, 123998, doi: 10.1016/j.apcatb.2024.123998.
[56] B. Hu, B. Wang, L. Chen, Z. Bai, W. Zhou, J. Guo, S. Shen, T. Xie, C. Au, L. Jiang, S. Yin, Electronic modulation of the interaction between Fe single atoms and $WO_{2.72-x}$ for photocatalytic N_2 reduction, *ACS Catalysis*, 2022, **12**, 11860-11869, doi: 10.1021/acscatal.2c03367.
[57] C. Feng, T. Bo, P. Maity, S. Zuo, W. Zhou, K.-W. Huang, O. F. Mohammed, H. Zhang, Regulating photocatalytic CO_2 reduction kinetics through modification of surface coordination sphere, *Advanced Functional Materials*, 2024, **34**, 2309761, doi: 10.1002/adfm.202309761.
[58] M. Ni, Y. Zhu, C. Guo, D.-L. Chen, J. Ning, Y. Zhong, Y. Hu, Efficient visible-light-driven CO_2 methanation with self-regenerated oxygen vacancies in $Co_3O_4/NiCo_2O_4$ hetero-nanocages: vacancy-mediated selective photocatalysis, *ACS Catalysis*, 2023, **13**, 2502-2512, doi: 10.1021/acscatal.2c05577.
[59] Z. Cheng, Y. Xu, B. Fei, Noble metal-free ternary cobalt-nickel phosphides for enhanced photocatalytic dye-sensitized hydrogen evolution and catalytic mechanism investigation, *RSC Advances*, 2023, **13**, 23638-23647, doi: 10.1039/d3ra04235a.
[60] S. Liu, W. Qi, J. Liu, X. Meng, S. Adimi, J. P. Attfield, M. Yang, Modulating electronic structure to improve the solar to hydrogen efficiency of cobalt nitride with lattice doping, *ACS Catalysis*, 2023, **13**, 2214-2222, doi: 10.1021/acscatal.2c05075.
[61] M. He, X. Zhang, S. Song, J. Yao, Z. Fang, W. Wang, X. Yuan, C. Li, H. Li, P. Li, W. Song, Z. Li, Tensile strain in tin oxide clusters stabilized by C_3N_4 for highly efficient visible light-driven H_2O_2 production, *ACS Sustainable Chemistry & Engineering*, 2022, **10**, 4494-4503, doi: 10.1021/acssuschemeng.1c08266.
[62] J. Xu, X. Zhang, W. Yan, T. Xie, Y. Chen, Y. Wei, Optimizing electronic density at active W sites for boosting photocatalytic H_2 evolution, *Inorganic Chemistry*, 2024, **63**, 4279-4287, doi: 10.1021/acs.inorgchem.3c04408.
[63] X. Qiao, Z. Wang, C. Li, H. Zhang, D. Hou, Y. Lan, D. Li, A new, efficient and durable MoO_2/Mo_2C-C cocatalyst with the optimized composition and electronic structure *via in situ* carburization for photocatalytic H_2 evolution, *Chemical Engineering Journal*, 2023, **455**, 140791, doi: 10.1016/j.cej.2022.140791.
[64] Z. Cheng, Y. Xu, B. Fei, Noble metal-free ternary cobalt-nickel phosphides for enhanced photocatalytic dye-sensitized hydrogen evolution and catalytic mechanism investigation, *RSC Advances*, 2023, **13**, 23638-23647, doi: 10.1039/d3ra04235a.
[65] B. Zhou, S. Xu, L. Wu, M. Li, Y. Chong, Y. Qiu, G. Chen, Y. Zhao, C. Feng, D. Ye, K. Yan, Strain-engineering of mesoporous $Cs_3Bi2Br_9/BiVO_4$ S-scheme heterojunction for efficient CO_2 photoreduction, *Small*, 2023, **19**, 2302058, doi: 10.1002/smll.202302058.
[66] J. Qiu, Y. Wu, S. Jiang, C. Sun, S. Song, Tuning *p*-band center of carbon nitride homojunction photocatalysts through strain effect for solar-driven H_2 production, *ACS Energy Letters*, 2023, **8**, 4173-4178, doi: 10.1021/acsenergylett.3c01779.
[67] X. Wu, F. Chen, N. Zhang, Y. Lei, Y. Jin, A. Qaseem, R. L. Johnston, Activity trends of binary silver alloy nanocatalysts for oxygen reduction reaction in alkaline media, *Small*, 2017, **13**, 1603387, doi: 10.1002/smll.201603387.
[68] V. R. Stamenkovic, B. Fowler, B. S. Mun, G. Wang, P. N. Ross, C. A. Lucas, N. M. Marković, Improved oxygen reduction activity on $Pt_3Ni(111)$ *via* increased surface site

availability, *Science*, 2007, **315**, 493-497, doi: 10.1126/science.1135941.
[69] Y. Pan, K. Sun, Y. Lin, X. Cao, Y. Cheng, S. Liu, L. Zeng, W. Cheong, D. Zhao, K. Wu, Z. Liu, Y. Liu, D. Wang, Q. Peng, C. Chen, Y. Li, Electronic structure and d-band center control engineering over M-doped CoP (M = Ni, Mn, Fe) hollow polyhedron frames for boosting hydrogen production, *Nano Energy*, 2019, **56**, 411-419, doi: 10.1016/j.nanoen.2018.11.034.
[70] G. Li, H. Liang, X. Fan, X. Lv, X. Sun, H. Wang, J. Bai, Modulating and optimizing 2D/2D Fe-$Ni_2P/ZnIn_2S_4$ with S vacancy through surface engineering for efficient photocatalytic H_2 evolution, *Journal of Materials Chemistry A*, 2023, **11**, 14809-14818, doi: 10.1039/D3TA02519E.
[71] Y. Zhou, W. Qin, X. Sun, Y. Zhu, J. Niu, Synergistic effects on d-band center *via* coordination sites of M-N3P1 (M = Co and Ni) in dual single atoms that enhances photocatalytic dechlorination from tetrachlorobispheonl A, *Journal of Hazardous Materials*, 2022, **430**, 128419, doi: 10.1016/j.jhazmat.2022.128419.
[72] H. Li, H. Ji, J. Liu, W. Liu, F. Li, Z. Shen, Interfacial modulation of $ZnIn_2S_4$ with high active Zr-S_4 sites for boosting photocatalytic activation of oxygen and degradation of emerging contaminant, *Applied Catalysis B*: *Environmental*, 2023, **328**, 122481, doi: 10.1016/j.apcatb.2023.122481.
[73] K. Chatterjee, A. Dutta, S. Mishra, B. Bairy, M. B. Sen, A. Gorai, S. K. Saha, A. J. Akhtar, Impact of tailoring of the defect states and the band gap towards extreme photocatalytic performance and photo-induced conductivity in cobalt doped ZnO QD, *Ceramics International*, 2023, **49**, 32768-32778, doi: 10.1016/j.ceramint.2023.07.245.
[74] X. Xiong, Y. Zhao, R. Shi, W. Yin, Y. Zhao, G. I. N. Waterhouse, T. Zhang, Selective photocatalytic CO_2 reduction over Zn-based layered double hydroxides containing tri or tetravalent metals, *Science Bulletin*, 2020, **65**, 987-994, doi: 10.1016/j.scib.2020.03.032.
[75] G. Qian, W. Lyu, X. Zhao, J. Zhou, R. Fang, F. Wang, Y. Li, Efficient photoreduction of diluted CO_2 to tunable syngas by Ni-co dual sites through d-band center manipulation, *Angewandte Chemie International Edtion*, 2022, **61**, e202210576, doi: 10.1002/anie.202210576.
[76] H. Guo, P. Yuan, J. Zhao, J. Zhao, Q. Peng, R. Song, First-principles studies of monolayers $MoSi_2N_4$ decorated with transition metal single-atom for visible light-driven high-efficient CO_2 reduction by strain and electronic engineering, *Chemical Engineering Journal*, 2022, **450**, 138198, doi: 10.1016/j.cej.2022.138198.
[77] S. Gong, B. Ni, X. He, J. Wang, K. Jiang, D. Wu, Y. Min, H. Li, Z. Chen, Electronic modulation of a single-atom-based tandem catalyst boosts CO_2 photoreduction to ethanol, *Energy & Environmental Science*, 2023, **16**, 5956-5969, doi: 10.1039/d3ee02643d.
[78] Y. Mao, M. Zhang, S. Si, G. Zhai, X. Bao, K. Song, L. Zheng, Y. Liu, Z. Wang, Z. Zheng, P. Wang, Y. Dai, H. Cheng, B. Huang, Electronic structure manipulation *via* site-selective atomically dispersed Ni for efficient photocatalytic CO_2 reduction, *ACS Catalysis*, 2023, **13**, 8362-8371, doi: 10.1021/acscatal.3c02000.
[79] P. Liu, B. Yang, Z. Xiao, S. Wang, S. Wu, M. Liu, G. Chen, X. Liu, R. Ma, N. Zhang, Engineering d-band states of $(CuGa)_xZn_{1-2x}Ga_2S_4$ material for photocatalytic syngas production, *Journal of Energy Chemistry*, 2023, **79**, 365-372, doi: 10.1016/j.jechem.2023.01.015.
[80] J. Xu, L. Lu, C. Zhu, Q. Fang, R. Liu, D. Wang, Z. He, S. Song, Y. Shen, Insights into conduction band flexibility induced by spin polarization in titanium-based metal-organic frameworks for photocatalytic water splitting and pollutants degradation, *Journal of Colloid and Interface Science*, 2023, **630**, 430-442, doi: 10.1016/j.jcis.2022.10.015.
[81] L. Xie, W. Huang, J. Chen, H. Chen, C. Hou, Q. Ni, T. Huang, L. Gui, X. Wang, Selective oxidation of β-keto ester modulated by the d-band centers in D-a conjugated microporous metallaphotoredox catalysts containing M-salen (MZn, Cu and Co) and triazine monomers, *Journal of Colloid and Interface Science*, 2024, **665**, 399-412, doi: 10.1016/j.jcis.2024.03.153.
[82] R. A. Borse, Y. X. Tan, J. Lin, E. Zhou, Y. Hui, D. Yuan, Y. Wang, Coupling electron transfer and redox site in boranil covalent organic framework toward boosting photocatalytic water oxidation, *Angewandte Chemie International Edtion*, 2024, **63**, e202318136, doi: 10.1002/anie.202318136.
[83] Y. Ma, Y. Zhang, G. Xie, Z. Huang, L. Peng, C. Yu, X. Xie, S. Qu, N. Zhang, Isolated Cu sites in CdS hollow nanocubes with doping-location-dependent performance for photocatalytic CO_2 reduction, *ACS Catalysis*, 2024, **14**, 1468-1479, doi: 10.1021/acscatal.3c05412.
[84] C. Yang, Y. Zhang, F. Yue, R. Du, T. Ma, Y. Bian, R. Li, L. Guo, D. Wang, F. Fu, Co doping regulating electronic structure of Bi_2MoO_6 to construct dual active sites for photocatalytic nitrogen fixation, *Applied Catalysis B*: *Environmental*, 2023, **338**, 123057, doi: 10.1016/j.apcatb.2023.123057.
[85] S. Gong, Y. Niu, X. Teng, X. Liu, M. Xu, C. Xu, T. J. Meyer, Z. Chen, Visible light-driven, selective CO_2 reduction in water by in-doped Mo_2C based on defect engineering, *Applied Catalysis B*: *Environmental*, 2022, **310**, 121333, doi: 10.1016/j.apcatb.2022.121333.
[86] J. Wang, C. Yang, L. Mao, X. Cai, Z. Geng, H. Zhang, J.

Zhang, X. Tan, J. Ye, T. Yu, Regulating the metallic Cu-Ga bond by S vacancy for improved photocatalytic CO_2 reduction to C_2H_4, *Advanced Functional Materials*, 2023, **33**, 2213901, doi: 10.1002/adfm.202213901.

[87] G. Dong, X. Huang, Y. Bi, Anchoring black phosphorus quantum dots on Fe-doped $W_{18}O_{49}$ nanowires for efficient photocatalytic nitrogen fixation, *Angewandte Chemie International Edition*, 2022, **61**, e202204271, doi: 10.1002/anie.202204271.

[88] Y. J. Lee, L. K. Putri, B. J. Ng, L. L. Tan, T. Y. Wu, S. P. Chai, Elucidating the enhanced decomposition of alkyl hydroperoxides on oxygen vacancy rich TiO_{2-x} surfaces using DFT for polyethylene decomposition, *Physical Chemistry Chemical Physics*, 2022, **24**, 25735-25739, doi: 10.1039/d2cp03768h.

[89] J. Zhao, Z. Xiong, J. Wang, X. Chen, J. Wan, Z. Xu, Y. Qiu, Y. Zhao, J. Zhang, Constructing bridging oxygen vacancies in $SnTa_2O_{6-x}$ for efficient and stable photocatalytic CO_2 reduction under visible light irradiation, *Applied Surface Science*, 2023, **636**, 157833, doi: 10.1016/j.apsusc.2023.157833.

[90] J. Wang, Y. Zhang, S. Jiang, C. Sun, S. Song, Regulation of *d*-band centers in localized CdS homojunctions through facet control for improved photocatalytic water splitting, *Angewandte Chemie International Edition*, 2023, **62**, e202307808, doi: 10.1002/anie.202307808.

[91] D. Wang, W. Wen, W. Li, G. He, C. Zhang, The doping of B in ZnO/CdS for enhanced visible-light H_2 production, *New Journal of Chemistry*, 2022, **46**, 14840-14848, doi: 10.1039/D2NJ01857H.

[92] H. Guo, H. Zhang, J. Zhao, P. Yuan, Y. Li, Y. Zhang, L. Li, S. Wang, R. Song, Two-dimensional WO_3-transition-metal dichalcogenide vertical heterostructures for nitrogen fixation: a photo(electro) catalysis theoretical strategy, *The Journal of Physical Chemistry C*, 2022, **126**, 3043-3053, doi: 10.1021/acs.jpcc.1c09772.

[93] F. Li, T. Huang, F. Sun, L. Chen, P. Li, F. Shao, X. Yang, W. Liu, Ferric oxide nanoclusters with low-spin FeIII anchored g-C_3N_4 rod for boosting photocatalytic activity and degradation of diclofenac in water under solar light, *Applied Catalysis B: Environmental*, 2022, **317**, 121725, doi: 10.1016/j.apcatb.2022.121725.

[94] C. Zhang, B. Liu, W. Li, X. Liu, K. Wang, Y. Deng, Z. Guo, Z. Lv, A well-designed honeycomb Co_3O_4@CdS photocatalyst derived from cobalt foam for high-efficiency visible-light H_2 evolution, *Journal of Materials Chemistry A*, 2021, **9**, 11665-11673, doi: 10.1039/D0TA11433B.

[95] H. Zhang, Q. Liu, Z. Shen, Highly efficient photocatalytic conversion of CO_2 into CH_4 over Cu single atom promoted heterojunction: The effect of uplifted d-band center, *Chinese Chemical Letters*, 2024, **35**, 108607, doi: 10.1016/j.cclet.2023.108607.

[96] F. Chen, L. Zhou, C. Peng, D. Zhang, L. Li, D. Xue, Y. Yu, Bimetal-organic layer-derived ultrathin lateral heterojunction with continuous semi-coherent interfaces for boosting photocatalytic CO_2 reduction, *Applied Catalysis B: Environmental*, 2023, **331**, 122689, doi: 10.1016/j.apcatb.2023.122689.

[97] Z. Lv, Y. Wang, Y. Liu, J. Wang, G. Qin, Z. Guo, C. Zhang, NiB as a substitute for the Pt cocatalyst in CdS with enhanced visible-light photocatalytic H_2 production, *The Journal of Physical Chemistry C*, 2022, **126**, 9041-9050, doi: 10.1021/acs.jpcc.2c01755.

[98] G. Wu, Z. Mo, P. Sun, Z. Cao, X. Zhu, Y. Song, Y. Wei, X. She, H. Li, H. Xu, Improved atomic hydrogen desorption by Cu_3N with suitable electronic structure to enhance photocatalytic H_2 evolution, *Materials Today Energy*, 2022, **29**, 101111, doi: 10.1016/j.mtener.2022.101111.

[99] Y. Zhang, Y. Dai, L. Yin, H. Li, X. Chen, B. Chen, Photocatalytic hydrogen evolution over nickel cobalt bimetallic phosphate anchored graphitic carbon nitrides by regulation of the d-band electronic structure, *Catalysis Science & Technology*, 2020, **10**, 3654-3663, doi: 10.1039/D0CY00556H.

[100] Q. Guo, F. Liang, Z. Sun, Y. Wang, X. Li, S. Xia, Z. C. Zhang, L. Huang, L. Wu, Optimal d-band-induced Cu_3N as a cocatalyst on metal sulfides for boosting photocatalytic hydrogen evolution, *Journal of Materials Chemistry A*, 2020, **8**, 22601-22606, doi: 10.1039/D0TA07916B.

[101] Y. Wu, M. Qu, S. Jiang, J. Zhang, S. Song, Synergistically regulating d-band centers of heterojunction redox sites by ligand effect for photocatalytic H_2 evolution, *Science China Materials*, 2024, **67**, 524-531, doi: 10.1007/s40843-023-2760-1.

[102] Y. Li, Q. Zhao, S. Liu, G. Ma, Y. Liu, R. Liu, H. Mu, X. Li, F. Li, Tuning electronic structure *via* CoS clusters for visual photocatalytic H_2 production and mechanism insight, *Chemical Engineering Journal*, 2022, **446**, 137399, doi: 10.1016/j.cej.2022.137399.

[103] Q. Zhang, Y. Xiao, Y. Li, K. Zhao, H. Deng, Y. Lou, J. Chen, L. Cheng, NiS-decorated ZnO/ZnS nanorod heterostructures for enhanced photocatalytic hydrogen production: insight into the role of NiS, *Solar RRL*, 2020, **4**, 1900568, doi: 10.1002/solr.201900568.

[104] D. Li, C. Liu, D. Huang, L. Wu, C. Li, W. Guo, Optimizing the d-band center of sub-nanometer Pd-Pt alloy clusters for improved photocatalytic dehalogenation of polyhalogenated biphenyls, *Separation and Purification*

Technology, 2024, **342**, 126887, doi: 10.1016/j.seppur.2024.126887.
[105] G. Wang, C. Zhang, W. Zhao, B. Wang, Y. Liu, T. Zhang, W. Cui, R. Zhang, Z. Zhao, Bonding interaction of adjacent Pt and Ag single-atom pairs on carbon nitride efficiently promotes photocatalytic H_2 production, *CCS Chemistry*, 2024, **6**, 1523-1534, doi: 10.31635/ccschem.023.202303154.
[106] L. Liu, P. Lv, DFT insight into the effect of Cu atoms on adsorption and dissociation of CO_2 over a Pd8/TiO_2(101) surface, *RSC Advances*, 2021, **11**, 17391-17398, doi: 10.1039/D1RA01724A.
[107] X. Cai, F. Wang, R. Wang, Y. Xi, A. Wang, J. Wang, B. Teng, S. Bai, Synergism of surface strain and interfacial polarization on Pd@Au core-shell cocatalysts for highly efficient photocatalytic CO_2 reduction over TiO_2, *Journal of Materials Chemistry A*, 2020, **8**, 7350-7359, doi: 10.1039/D0TA01247E.
[108] L. Liu, P. Lv, Understanding the enhanced catalytic activity of bimetallic AuCu/TiO_2 in CO_2 adsorption and activation: a density functional theory study, *New Journal of Chemistry*, 2020, **44**, 14662-14669, doi: 10.1039/D0NJ02266G.
[109] R. Long, Y. Li, Y. Liu, S. Chen, X. Zheng, C. Gao, C. He, N. Chen, Z. Qi, L. Song, J. Jiang, J. Zhu, Y. Xiong, Isolation of Cu atoms in Pd lattice: forming highly selective sites for photocatalytic conversion of CO_2 to CH_4, *Journal of the American Chemical Society*, 2017, **139**, 4486-4492, doi: 10.1021/jacs.7b00452.
[110] W. Zhang, Q. Li, H. Xia, Photocatalytic oxidation of 5-hydroxymethylfurfural to furandicarboxylic acid over the Au-Ag/TiO_2 catalysts under visible light irradiation, *Applied Surface Science*, 2023, **613**, 156036, doi: 10.1016/j.apsusc.2022.156036.
[111] S. Han, X. Qi, W. Zhang, X. Li, D. Liu, $AuGa_2$-based plasmonic nanocomposite with engineered d-band for enhanced photocatalytic and antibacterial activities, *Journal of Alloys and Compounds*, 2023, **934**, 167945, doi: 10.1016/j.jallcom.2022.167945.
[112] W. Zhang, Q. Peng, L. Shi, Q. Yao, X. Wang, A. Yu, Z. Chen, Y. Fu, Merging single-atom-dispersed iron and graphitic carbon nitride to a joint electronic system for high-efficiency photocatalytic hydrogen evolution, *Small*, 2019, **15**, 1905166, doi: 10.1002/smll.201905166.
[113] T. Lv, B. Xiao, F. Xia, M. Chen, J. Zhao, Y. Ma, J. Wu, J. Zhang, Y. Zhang, Q. Liu, Insights into synergistic effect of Pd single atoms and sub-nanoclusters on TiO_2 for enhanced photocatalytic H_2 evolution, *Chemical Engineering Journal*, 2022, **450**, 137873, doi: 10.1016/j.cej.2022.137873.
[114] G. Liu, Y. Zhu, H. Gao, S. Xu, Z. Wen, L. Sun, F. Li, Photocatalytic water oxidation by surface modification of $BiVO_4$ with heterometallic polyphthalocyanine, *ACS Catalysis*, 2023, **13**, 8445-8454, doi: 10.1021/acscatal.3c01235.
[115] N. Liu, J. Jiang, Z. Chen, B. Wu, S. Zhang, Y. Zhang, P. Cheng, W. Shi, Promoted photocatalytic hydrogen evolution by tuning the electronic state of copper sites in metal-organic supramolecular assemblies, *Angewandte Chemie International Edition*, 2023, **62**, e202312306, doi: 10.1002/anie.202312306.
[116] Y. Liu, L. Li, H. Tan, N. Ye, Y. Gu, S. Zhao, S. Zhang, M. Luo, S. Guo, Fluorination of covalent organic framework reinforcing the confinement of Pd nanoclusters enhances hydrogen peroxide photosynthesis, *Journal of the American Chemical Society*, 2023, **145**, 19877-19884, doi: 10.1021/jacs.3c05914.
[117] X. Wang, K. Huang, W. Ma, Y. Cong, C. Ge, S. Feng, Defect engineering, electronic structure, and catalytic properties of perovskite oxide $La_{0.5}Sr_{0.5}CoO_{3-\delta}$, *Chemistry-A European Journal*, 2017, **23**, 1093-1100, doi: 10.1002/chem.201604065.
[118] A. Dey, G. Chandrabose, L. A. O. Damptey, E. S. Erakulan, R. Thapa, S. Zhuk, G. K. Dalapati, S. Ramakrishna, N. S. J. Braithwaite, A. Shirzadi, S. Krishnamurthy, Cu_2O/CuO heterojunction catalysts through atmospheric pressure plasma induced defect passivation, *Applied Surface Science*, 2021, **541**, 148571, doi: 10.1016/j.apsusc.2020.148571.
[119] C. C. Er, L. K. Putri, B. J. Ng, J. Y. Tang, N. V. Medhekar, S. P. Chai, Allotropes selection apropos of photocatalytic CO_2 reduction from first principles studies, *Materials Today Physics*, 2022, **26**, 100751, doi: 10.1016/j.mtphys.2022.100751.
[120] X. Zhang, F. Wu, G. Li, L. Wang, J. Huang, A. Meng, Z. Li, Modulating electronic structure and sulfur p-band center by anchoring amorphous Ni@NiS_x on crystalline CdS for expediting photocatalytic H_2 evolution, *Applied Catalysis B: Environmental*, 2024, **342**, 123398, doi: 10.1016/j.apcatb.2023.123398.